AN ANALYSIS OF THE EFFECT OF HIGH CONGESTION RATES IN PHILIPPINE PRISONS ON SARS-COV-2 PROPAGATION USING SEIR AGENT-BASED MODELING APPROACH

BY

Chien Carisse P. Fernandez

A special problem submitted to the

Department of Mathematics and Computer Science

College of Science

The University of the Philippines

Baguio, Baguio City

as partial fulfillment of the

requirements for the degree of

Bachelor of Science in Computer Science

June 2023

This is to certify that this Special Problem entitled **"AN ANALYSIS OF THE EFFECT OF HIGH CONGESTION RATES IN PHILIPPINE PRISONS ON SARS-CoV-2 PROPAGATION USING SEIR AGENT-BASED MODELING APPROACH"**, prepared and submitted by **Chien Carisse P. Fernandez** to fulfill part of the requirements for the degree of **Bachelor of Science in Computer Science**, was successfully defended and approved on June 16, 2023.

Joel M. Addawe, Ph.D.
Special Problem Adviser

The Department of Mathematics and Computer Science endorses the acceptance of this Special Problem as partial fulfillment of the requirements for the degree of Bachelor of Science in Computer Science .

Gilbert R. Peralta, Dr.rer.nat
Chair
Department of Mathematics and
Computer Science

Table of Contents

Acknowledgments

This undergraduate thesis is by no means a product of my singular effort. It is also a product of the individuals who helped me grow academically, intellectually, and emotionally during this research and throughout my life. I dedicate this thesis to all of you. This study was only possible with the exceptional patience and assistance of my adviser, Prof. Joel M. Addawe. Your academic guidance and advice in each of my consultations greatly benefited my work. From the start of my thesis journey, you remained my adviser and afforded me patience and understanding. To my course adviser Prof. Ashlyn D. Balangcod, your patience and guidance provided me encouragement right from my freshman year until the fourth year of my stay at the university. Next, I largely attribute my academic growth to the College of Science, the professors I had in my whole undergraduate degree, and all the staff. The UPB community creates warmth much needed in the chill cold of the city and I can only be honored to be a part of it for the past four years. I wish to thank the Philippine Bureau of Corrections for taking the time to provide the data I needed to accomplish this study. My biggest debt, however, is to my family. My parents, Alicia and Eduardo, thank you for taking good care of me, building a home amidst life's adversities, and always reminding me of my potential. My sisters, Candace, Denise, and Chynna, you all motivate me and make me proud. Yujin, Crumpy, and Max thank you for keeping me sane throughout the writing of this thesis. My deepest thanks also go to Ate Nars who has been my partner in this thesis journey. The genesis of this thesis would not have been formulated without your generous help. I also want to express my appreciation to my best friend, Myla. I deeply appreciate your help and unwavering faith in me. Finally, I know that I would be able to finish my thesis without the constant motivation from my biggest cheerleader, Neo. Thank you for your clever ways of encouraging me when times are rough. Onto our next adventure!

Abstract

AN ANALYSIS OF THE EFFECT OF HIGH CONGESTION RATES IN PHILIPPINE PRISONS ON SARS-CoV-2 PROPAGATION USING SEIR AGENT-BASED MODELING APPROACH

Chien Carisse P. Fernandez
University of the Philippines, 2023

Adviser:
Joel M. Addawe, Ph.D.

Philippine prisons have been epicenters of diseases as a consequence of severe overcrowding, inaccessible healthcare, and poor sanitation and ventilation systems. With the escalation of the novel coronavirus COVID-19 infection worldwide, enclosed and congested spaces such as prison facilities are extremely vulnerable to high infection rates. Thus, this study examines the effect of high congestion rates in Philippine prisons on the propagation of the COVID-19 disease and generated the proper set of health protocols that should be administered to mitigate the spread. An agent-based model is developed to mimic the infection transmission dynamics inside prison facilities. Scenario-based experiments are conducted to evaluate the effectiveness of different nonpharmaceutical interventions including mask use, different levels of lockdown intensities and limited activity. Simulations were executed using parameters that adhere to the recommended prison condition and maximum capacity, and parameters that represent the actual prison condition and population in 2020. The research findings suggest that the use of facemasks has the most significant impact in reducing the infection rate by 39.33%. A total lockdown on the first day of the outbreak must also be implemented to reduce the chances of passing the infection to other prison cells. Another mobility restriction that must be qualified is limiting the movement of the persons deprived of liberty (PDLs) by 50%. If these health protocols are administered properly, the infection rates can reduce by 73.15%.

List of Tables

List of Figures

Chapter 1

Introduction

1.1 Background of the Study

Extreme congestion, limited access to healthcare, inadequate cleanliness and ventilation systems are the major problems of Philippine prisons, putting them at elevated risk during the COVID-19 pandemic. The novel coronavirus COVID-19 infection was rapidly spreading throughout the world starting from the year 2020, making enclosed and crowded areas like jail facilities particularly susceptible to high infection rates. In March 2020, around the time the first COVID-19 lockdown was imposed in the country, the Bureau of Corrections reported that 125 prisons were at 310% occupancy rate in January 2020 [53]. The virus can spread from one host to another through different modes such as coughing, sneezing, talking or through fomite transmission by getting the infection through contaminated surfaces. When a person gets infected, symptoms such as fever, cough, fatigue, and loss of taste can appear after 5 to 6 days of getting infected [45]. Since the COVID-19 virus predominantly spread through airborne transmission and close contact, people inside congested and poorly ventilated spaces are all at severe risk of contracting the virus.

The virus is considered to be highly transmissible [24] and this high transmission rate alarms the government in most countries, hence, in the absence of vaccines particularly equipped for ceasing the spread of the virus, governments worldwide have employed non-pharmaceutical interventions and conducted extensive search operations to detect active cases. Contact tracing was also used to identify people in close contact with an infected host. Serious cases were admitted to hospitals while those with minor symptoms were confined at home or taken to specialized isolation facilities. A number of restrictions were implemented to prevent the disease from spreading further, including the closing of public spaces like parks and schools, the suspension of international flights and local transport,

restricted economic activities, maintenance of physical distancing, and the prescription of face masks.

However, this system of strategies is not apt or enough for congested spaces such as municipal jails and large-scale correctional facilities. Moreover, considering that the Philippines has the highest jail congestion rate in the world [20], it is extremely challenging to implement the proper interventions to mitigate the spread of the virus. In consideration of that fact, this paper aims to evaluate the spread of SARS-CoV-2 inside correctional facilities in the country and investigate the effect of different non-pharmaceutical interventions. The results further discuss the proper strategies that are recommended to stabilize the transmission of COVID-19 inside the correctional facilities of the country.

This study includes four sections. The second section deals with the literature review of studies related to the COVID-19 pandemic, prison conditions in the Philippines, and agent-based modeling. The third part gives detailed information about the methodology of the study. The results obtained from the method and the implemented agent-based model are discussed in the fourth section. In the last section, a conclusion and recommendations for future directions about the study have been provided.

1.2 Statement of the Problem

People who are detained or who work in correctional settings are at elevated risk for exposure to COVID-19 [4]. Philippine correctional facilities and jails are highly congested, have poor sanitation and inaccessible healthcare system. These factors pose an additional challenge to preventing the escalation of the disease.

With the declaration of the pandemic, the fragile health systems of the prison facilities became paralyzed. However, the decongestion process of these facilities demands extensive time and resources. Given that the outbreak of the SARS-CoV-2 cases is sudden and that the Philippine government has deficient resources to subsidize the expansion of facilities to house the rising number of persons deprived of liberty (PDL), it is challenging to resolve this catastrophic problem immediately.

Hence, considering the current congestion rate of correctional facilities in 2020, the research findings will contribute to developing an apt set of strategies for stabilizing and

preventing outbreaks inside congested prison spaces.

1.3 Objective of the Study

1.3.1 General Objective of the Study

This study aims to determine the appropriate synthesis of strategies and non-pharmaceutical interventions to alleviate the upsurge of COVID-19 inside correctional facilities in the Philippines.

1.3.2 Specific Objective of the Study

1. To develop an agent-based model that visualizes the spread of COVID-19 inside prison facilities in the Philippines as a result of each PDL's interaction and mobility behavior in a geospatial context;

2. To compare the transmission of the COVID-19 disease inside the correctional facilities under the Bureau of Corrections when the population of the PDLs is at the facility's recommended maximum capacity and when the population of the PDLs is at the facility's actual occupancy rate in 2020;

3. To measure the decrease in COVID-19 infection rates when mandatory use of face masks is implemented;

4. To evaluate the effect of the different levels of intensities of lockdown policies on the decrease of infection rates; and

5. To assess the decrease in COVID-19 infection rates when the movement of the PDLs is limited.

1.4 Significance of the Study

The goal of this study is to simulate the evolution of the COVID-19 outbreak inside congested spaces based on real-world containment strategies. These protocols include the common nonpharmaceutical interventions that governments around the world such as the mandatory use of face masks, lockdown protocols, and mobility restrictions.

Moreover, the results of this study will suggest suitable interventions for the current congestion conditions of the Philippine prisons that are validated by statistical data. Consequently, the model enables forecasts on the propagation of COVID-19 by reporting predictions for significant indices. The created model is highly adaptable to different parameters which permits the deletion or inclusion of constraints like rules and nonpharmaceutical interventions. The model investigates the spread of the infection over time, which presents the opportunity to proceed in forecasting further simulations during the COVID-19 pandemic or help prevent other diseases that may spread inside the Philippine prisons.

Recent studies for agent-based modeling of SARS-CoV-2 focused on the evolution of contagion of the disease in specific cities [13, 15, 43, 47], and the effectiveness of different nonpharmaceutical interventions to mitigate its evolution [6, 52]. However, few to no studies have focused on the transmission of the COVID-19 disease inside the prison facilities which are housing one of the most vulnerable populations in times of pandemic. This model differs from other agent-based models for COVID-19 spread as it analyzes the conditions inside prisons and develops appropriate plans to prevent the spread of transmissible diseases inside these congested spaces.

1.5 Scope and Limitation

There are different types of prisons under different agencies of the Philippine government that are in 2.3. However, for this paper, only the seven correctional facilities under the Bureau of Corrections will be considered. Hence, this study does not include the small-scale provincial and municipal jails around the country since these spaces have different specifications for prison cell buildings and parameters. Additionally, this study

focused on the recorded statistical data given by the Bureau of Corrections at the first outbreak of the virus in 2020.

Chapter 2

Preliminaries

The concepts of agent-based modeling and its use on epidemiological levels will be elaborated in this section. Research works on the use of agent-based models to simulate COVID-19 transmission using real-life data will also be discussed. It will be followed by the current Philippine prison conditions and the timeline of control measures that have been implemented during the pandemic. Overall, this section will present a foundation of knowledge on the topic to support the problem, methods, and results of the study.

2.1 Agent-Based Modeling

Agent-based model is a type of computer simulation consisting of agents that interacts with one another within an environment. The agents' interactions and actions are governed by a set of programmed rules [18]. Since agents can stochastically make their own decisions within the model based on the prescribed rules, the model captures unexpected collective phenomena resulting from a combination of individual behaviors of the model.

Agent-based models (ABMs) are a class of computational models based on computer simulations that simulate the activities and interactions of autonomous agents in order to assess how these interactions affect the system as a whole. The agent-based approach places a strong emphasis on learning through the interactions between agents and their environments. This strategy fits into a recent trend in computational models of learning that aims to create fresh approaches for researching autonomous agents in either virtual or actual contexts [17].

Agent-based simulation modeling has been used primarily in epidemiological studies of infectious diseases. Some of these studies include the evaluation of the effect of chickenpox vaccination on shingles epidemiology [38], the study on the propagation of influenza in Egypt [21], and the study of the spread of malaria in Niger [39].

In order to better plan for future outbreaks, other models in some studies are being utilized to explain previous outbreaks. These studies include the model on the 2014 Ebola outbreak in Liberia [25] and the model on the H1N1 outbreak in Mexico City [12]. The research findings of these studies are used to evaluate preventative measures and responses before a pandemic occurs.

2.1.1 Compartmental Models

The compartmental model is a modeling technique that is commonly used in the field of epidemiology. In these models, the population is assigned to compartments such as susceptible, exposed, infectious, recovered, or deceased. The individuals may progress between these compartments depending on the programmed rules. The model can be implemented using deterministic differential equations (equation-based model) or a stochastic framework (agent-based model).

Equation-based models provide adequate results in understanding complex systems and predicting behaviors by adjusting coefficients. However, it is challenging to fit different intervention schemes into a single equation-based model that can be able to quantify the efficacy of different strategies that are concurrently applied. In an agent-based model, the effect of the environmental conditions and adding parameters for intervention strategies is highly reflected on an individual level [45].

This section will illustrate the different compartmental models used in epidemiology and discuss their equation-based differential framework. The differential equations in this section will present the change of the number of the population over unit time t.

Susceptible-Infected (SI) Model

The Susceptible-Infected (SI) model is one of the simplest models that describes the spread of an infectious disease in a population. The model assumes that individuals in the population are only either susceptible to contracting the disease or are already infected. In most experiments, this is used to survey the period until the susceptible population is exhausted and all became infectious. The susceptible population is represented by **S** while the infected population is represented by **I**.

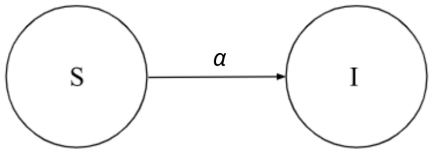

Figure 2.1: Illustration for the progression of the states of Susceptible-Infected Compartmental Model

Figure 2.1 illustrates the progress of the infection states of the agents for the SI model. The rate of transmission at which susceptible agents become infected is given by α. The following differential equations governed the SI model.

$$\frac{dS}{dt} = -\alpha \mathbf{SI}$$
$$\frac{dI}{dt} = \alpha \mathbf{SI}$$

In the illustration, the infection state starts with susceptible. An agent can be infected at a certain time t with an infection rate α. The change in the number of susceptible people as time progresses is represented by $\frac{dS}{dt}$ while the change in the infected population over time is represented by $\frac{dI}{dt}$.

Susceptible-Infected-Recovered (SIR) Model

Compared to the SI model, the SIR model assumes that the population can have the following infection state: susceptible, infected, and recovered. The added compartment 'recovered' is represented by **R**. This represents the population that was once infected by the disease then recovered and became immune to contracting the disease.

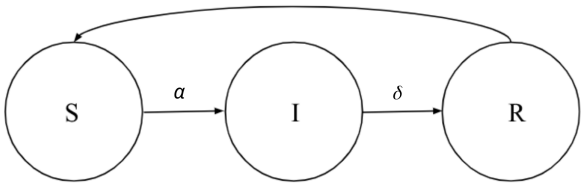

Figure 2.2: Illustration for the progression of the states of Susceptible-Infected-Recovered Compartmental Model

Figure 2.2 illustrates the progress of the infection states of the agents for the SIR model with **S** representing the susceptible state, **I** as the infectious state and **R** as the recovered state. In the illustration, a susceptible individual can be infected based on the infection rate α. An infected agent can change its state to a recovered state by the δ recovery rate. The recovered individuals will eventually become susceptible again or stay in their recovered and immune state, depending on the programmed rules of the agent-based model. The infection rate is represented by α and the rate recovery rate is δ. The equation-based differential equations counterpart for SIR is as follows:

$$\begin{aligned}\frac{dS}{dt} &= -\alpha \mathbf{SI} \\ \frac{dI}{dt} &= \alpha \mathbf{SI} - \delta \mathbf{I} \\ \frac{dR}{dt} &= \delta \mathbf{I}\end{aligned}$$

To evaluate the change in the population that has recovered from the disease, the formula is given by $\frac{dR}{dt}$.

Susceptible-Exposed-Infected-Recovered (SEIR) Model

For an SEIR model, an agent starts as being susceptible to the disease. If it was brought in contact with an infected one, it will progress to an exposed state. Depending

on the programmed rules, the agent can progress to being infected or be back to its susceptible state. After infection, it will recover and be back again to being susceptible to contracting the disease.

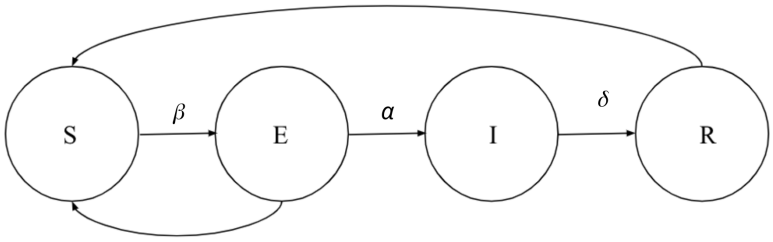

Figure 2.3: Illustration for the progression of the states of Susceptible-Exposed-Infected-Recovered Compartmental Model

Figure 2.3 presents the progression of the states for the SEIR model. The added exposed compartment is represented by **E** while the exposure, infection rate and recovery rate are represented by β, α and δ, respectively. The following differential equations can be used to compute these rates in an equation-based model.

$$\begin{aligned}
\frac{dS}{dt} &= -\beta \mathbf{SI} \\
\frac{dE}{dt} &= \beta \mathbf{SI} - \alpha \mathbf{E} \\
\frac{dI}{dt} &= \alpha \mathbf{E} - \delta \mathbf{I} \\
\frac{dR}{dt} &= \delta \mathbf{I}
\end{aligned}$$

Susceptible-Exposed-Infected-Recovered-Deceased (SEIRD) Model

The SEIRD model is an extension of the SEIR model in which the emphasis on the outcome after infection is added. In this model, the infected agent can recover be immune

to the infection, or can be removed from the population due to death brought on by the disease.

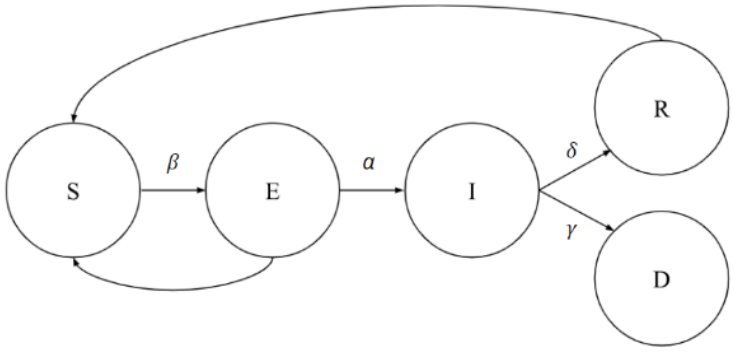

Figure 2.4: Illustration for the progression of the states of Susceptible-Exposed-Infected-Recovered-Deceased Compartmental Model

The SEIRD compartmental model is governed by differential equations where **S** is the total number of susceptible agents from the total population, **E** is the number of agents who have been exposed to an infected agent but are not yet infectious, **I** represents the population of the infected agents who are currently infectious, **R** is the number of in recovered agents and is immune to the disease, and **D** represents the population of the agents who have died from the disease. Thus, it follows that

$$\begin{aligned}
\frac{dS}{dt} &= -\beta \mathbf{SI} \\
\frac{dE}{dt} &= \beta \mathbf{SI} - \alpha \mathbf{E} \\
\frac{dI}{dt} &= \alpha \mathbf{E} - (\gamma + \delta)\mathbf{I} \\
\frac{dR}{dt} &= \gamma \mathbf{I} \\
\frac{dD}{dt} &= \delta \mathbf{I}
\end{aligned}$$

The above parameters are defined as β to be the rate at which susceptible agents become exposed, α is the infection rate at which exposed agents become infectious, δ as the recovery rate, and γ as the mortality rate. The differential equations show the change of each compartment's population over time as functions of the given rates.

2.1.2 Agent-Based Modeling in COVID-19

Amidst the outbreak of COVID-19, numerous studies utilized an agent-based modeling approach to simulate the propagation of the virus in a spatiotemporal context. Most of these model aims to infer the proper set of nonpharmaceutical strategies to stem the spread of the COVID-19 virus. One study in France founds the great potential impact of post-lockdown measures, including physical distancing, mask-wearing, and shielding individuals who are the most vulnerable to severe infection in mitigating the propagation of the virus [15]. A study in the Philippines used the agent-based modeling approach to study the spread of the virus inside Philippine classrooms and infer the best classroom setup to minimize the risk of transmission [23]. These studies were used to inform policymakers throughout the world of the expected behavior of the COVID-19 outbreak and the proper interventions that must be administered to stem the virus from propagating at higher levels.

2.2 COVID-19

The COVID-19 disease is a highly contagious viral infection caused by a zoonic novel syndrome coronavirus 2 (SARS-CoV-2). Similar to the other two coronaviruses like SARS-CoV 1 and MERS-CoV, SARS-CoV-2 is likely to have originated from bats, which are known as an established natural reservoir for many various pathogens [22]. Being a zoonic virus, coronaviruses have the capability to transfer from animals to humans and spread it to other humans through airborne aerosols [50]. Droplet transmission of SARS-CoV-2 occurs when a person is within one-meter distance of a person who has respiratory symptoms such as coughing, sneezing, or talking. The mean infectious period for symptomatic cases is 13.4 days while the potential maximum infectious period is 18.1 days [9]. The virus may be spread by the infected host through conductive (eyes), mucosae (mouth and nose), or fomite transmission (through contaminated surfaces). Though mucosal transmission is the most frequent, conjunctival transmission of the virus through conjunctiva is relatively less common [34]. Moreover, similar to other coronaviruses, SARS-CoV-2 may spread by environmental pollution, which could lead to

nosocomial outbreaks.

The novel coronavirus outbreak originated in Wuhan, China and has spread to numerous other countries. The first documented case of atypical pneumonia linked to SARS-CoV-2 in China was at the end of 2019 [44]. On January 30, 2020, the World Health Organization Emergency Committee declared a global health emergency due to rising case notification rates at Chinese and international locations [51]. It was then elevated to its status and was declared a pandemic by the World Health Organization in March 2020.

One study provided evidence that even though COVID-19 has a lower mortality rate than other coronaviruses such as MERS-HCoV (approximately 40% mortality rate) and SARS-HCoV (approximately 10% mortality rate), its high transmissibility produces a higher death rate in terms of absolute terms [36]. Moreover, despite the low fatality and morbidity rates of SARS, the pandemic's effects on health extended beyond those who were infected. The novelty of causing virus, the capability of rapid nosocomial transmission, and the susceptibility of hospitals and healthcare personnel did in fact greatly increase great fear among the general population [11].

2.2.1 COVID-19 outbreak in the Philippines

The first reported COVID-19 case in the Philippines was on 30 January 2020. The Philippine Department of Health confirmed the patient as a 38-year-old female Chinese national. On 1 February 2020, the Philippine Department of Health confirms the first COVID-19 death in the Philippines however, the Philippine government does not take any significant action to prepare for the potential growth of the COVID-19 disease.

On March 7, the first local transmission of COVID-19 was confirmed hence the following day, on March 8, Philippine President Duterte declares a state of public emergency to stem the increasing number of COVID-19 infections, especially in Metro Manila. On 12 March 2020, community quarantine was implemented throughout the entirety of Metro Manila. The authorities hurried to curb the transmission of COVID-19. Domestic travels through air, land and sea are banned.

On March 16, a few days after Duterte placed Metro Manila under a state of quarantine, he subsequently decided to put the entire Luzon under an enhanced community quarantine (EQQ). Under this quarantine rule, "strict home quarantine shall be implemented in all households; transportation shall be suspended; provision for food and essential services shall be regulated, and heightened presence of uniformed personnel to enforce quarantine procedures will be implemented."

In 2020, the Philippines recorded 474,064 COVID-19 cases, 439,796 recoveries, and 9,244 fatalities [7].

2.2.2 Nonpharmaceutical Interventions

In the first 12 months of the COVID-19 emergency and in the absence of vaccines, each community's only weapon against the COVID-19 disease was non-pharmaceutical interventions (NPIs). The term "NPIs" refers to a broad variety of top-down (i.e., governmental) and bottom-up (i.e., self-initiated) actions intended to stem the transmission of infections by changing key facets of human behavior. Examples of NPIs include travel restrictions, curfews, social isolation, social gathering bans, mandatory use of face masks, improved hygiene and cleanliness, remote working, school closures, and lockdowns [35].

Numerous studies aimed to measure the efficiency of NPIs. The modeling efforts of these studies consistently illustrate the significance and effectiveness of NPIs in controlling the spread of COVID-19 [35]. The timely implementation of NPIs is significant to their success. This means finding a balance between implementing the control measures early enough to prevent the epidemic's peak and long enough to allow for their maintenance [19].

Use of face masks

One of the most popular NPIs that have been introduced in practically all nations as the first line of defense against COVID-19 disease is the mandatory use of face masks. Numerous studies compare the usage of face masks, irrespective of the type, with the absence of face masks. In these studies, it was found that those who did not use masks had much higher infection rates [2]. A study conducted in Germany examined the impact

of the use of face masks to control the COVID-19 outbreak. Their estimations concluded that face masks reduce the chance of getting infected by around 47% [26].

On 2 April 2020, the Philippine government implemented a policy to mandate the use of face masks or other forms of protective equipment for places under the Enhance Community Quarantine (ECQ), particularly in Luzon, where a month-long curfew was imposed [32].

Lockdowns and mobility restrictions

Social distancing is one of the most significant NPIs control actions that can curb the spread of the highly contagious COVID-19 disease and lockdown is at the forefront of these social distancing restrictions. One study used a Susceptible-Infected-Recovered/Removed (SIR) agent-based model to investigate the impact of lockdown strategies and mobility patterns on the propagation of COVID-19. The paper's key finding is that closing schools is the most effective way to quantitatively reduce the daily incidence of COVID-19, followed by postponing public events and placing limits on private meetings. Workplace and stay-at-home obligations come next, however, their statistical significance and levels of impact are not as strong. Instead, the researchers discovered no impact of international travel restrictions, closures of public transportation, or limitations on movement between cities and regions [5]. Another research work in 2020 studied the impact of social restrictions in 37 countries and found that societal mobility restrictions appear to have reduced COVID-19 spread in many countries, especially during the first waves of the epidemic, but the magnitude of the impact is reduced in the late phase once further mitigating measures have been implemented [30].

2.3 Philippine Prisons

There are different types of prison building specifications under the Philippine government. The Bureau of Jail and Penology is an agency under the watch of the Department of the Interior and Local Government. In accordance with the Republic Act No. 6975, this agency exercises supervision and management of every city and municipal jail in the country. These jails house temporarily confined prisoners who are detained awaiting

investigation, trial or transfer to the national penitentiary, and violent mentally ill person who endangers himself or the safety of others and who is pending transfer to a mental institution [28].

On the other hand, the Bureau of Corrections is an agency under the Department of Justice which is responsible for the custody and rehabilitation of PDLs who have been sentenced to three or more years of imprisonment. According to the Bureau of Corrections Act of 2013, the agency aims to effectively safekeep and rehabilitate national prisoners. Its vision is to have improved national prisons that are able to reform and rehabilitate PDLs and reintegrate them back into society as contributing citizens of the country [27]. As stated in the constraints of this study, the results only focused on the prison conditions and statistical data from the Bureau of Corrections. The correctional facilities under Bureau of Coreections are:

1. New Bilibid Prison;
2. Correctional Institute for Women - Mandaluyong;
3. Iwahig Prison and Penal Farm;
4. Davao Prison and Penal Farm;
5. San Ramon Prison and Penal Farm;
6. Sablayan Prison and Penal Farm; and
7. Leyte Regional Prison.

2.3.1 Ideal Prison Specifications

As a background of the term based on the Mandela Rule, prisoners are referred to as persons deprived of liberty (PDLs) and are guaranteed minimum humanitarian treatment [10]. The term PDLs is adopted to avoid branding the use of disparaging terms like "prisoner" and others in accordance with Article 10 of the International Covenant on Civil and Political Rights, which guarantees respect for the fundamental dignity of the human person. In the Philippines, the new term PDL was legally defined as "detainee,

inmate, or prisoner or other person under confinement or custody in any other manner" by Section 23 of Republic Act 10575 [27]. Moreover, under Section 7 of the same Republic Act, the following parameters and building specifications for prison cells must be followed:

Cell Building Feature	**Ideal Parameter Specification**
Habitable floor area per PDL	4.7 square meters
Maximum number of PDLs per cell	10 PDLs
Maximum number of two-level bunk beds	5 units
Wash area (for utensils, hand washing)	1 unit
Water closet (toilet bowl)	1 unit
Bath area	1 unit

Table 2.1: The recommended standard layout and building specifications for prison cell dormitories of the Bureau of Corrections [27]

An efficient criminal justice system is necessary for a nation's national security development. The humane treatment of PDLs and their preparation for reintegration after release are key measures for an effective justice system. In line with the Bureau of Correction's mission to safekeep and institute reformation programs for national PDLs, the agency's facilities must be congruent with this agenda. However, in many cases, these aims of expiation and reformation are not served.

2.3.2 Prison Conditions

A number of studies and reports have focused on the challenges inside the correctional facilities of the country. As reported by the International Committee of the Red Cross, the Philippines has the highest congestion rate worldwide [29]. The statistical data provided by the Bureau of Corrections presents that the average congestion rate in the seven correctional facilities under the agency in 2020 is 358%.

This severe congestion status has gotten worse due to the high and abrupt influx of PDLs detained in connection with the anti-drug effort since July 2016, as documented by the Commission on Human Rights of the Republic of the Philippines. Other factors for the high congestion rates in city and municipal jails under BJMP include the inability

of detainees to post bail, poor case disposition or protracted trials, undersized lock-up cells, and delays in the issuance of commitment orders [8].

These factors further aggravate the overcrowding challenge worse, which has a significant impact on the living conditions and accessibility of PDLs to essential services such as water, sanitation and healthcare. In the initial outbreak of COVID-19 in the country, there has been a public expression of increased concerns that the spaces occupied by the PDLs may soon become epicenters of the COVID-19 infection due to the upward trend in the country's prison population, which is exacerbated by the correctional facilities' appalling structural condition [41].

2.3.3 COVID-19 outbreak inside Philippine Prisons

On 10 March 2020, amid the outbreak of COVID-19 in the country, the Bureau of Jail Management and Penology activated the "Oplan 2019 Novel Coronavirus" which addresses security measures for the 468 Philippine jails. On the following day, visitation rights were suspended in almost all regions in Luzon.

To avoid the virus from entering the prisons, the Bureau of Jail Management and Penology stopped accepting detainees from police lockup cells. On 15 March 2020, an organization called "Kapatid" appeals for the release of low-level offenders, sick, elders, and political PDLs. In the same week, an absolute lockdown was imposed, barring visitation and the handling of food and meals to PDLs in all jails.

Two inmates for the Correctional Institute for Women in Mandaluyong were taken to hospitals, both were swabbed and tested positive for COVID-19. It was 17 April 2020 when it was reported that COVID-19 exploded inside Philippine jails and prisons. The first death related to COVID-19 was on 19 April 2020 which was an inmate in Cebu City jail [42].

2.3.4 COVID-19 Response in Philippine Correctional Facilities

Amid the COVID-19 crisis, the United Nations Office on Drugs and Crime has released a position paper for the protection of the constrained population of PDLs as well as staff members and police who are involved in ensuring their custody [31]. The paper

emphasized the PDLs' rights to receive equal healthcare standards and recommended the adoption of substitute policies without compromising their legal status. It further urged the government of countries worldwide to address the overcrowded prisons and ease imprisonment measures.

In April 2020, the Human Rights Watch urges the Philippine government to immediately reduce the PDL population housed in the overcrowded prisons to stem the COVID-19 outbreak. The Human Rights Watch particularly recommends the release of PDLs who have been detained or convicted for low-level and non-violent offenses and prioritizes the release of older prisoners and those with underlying medical conditions who would be at greater risk if they became infected [53].

The study of Cahapay 2020 [10] discusses the national responses for PDLs during the COVID-19 pandemic in the country. The paper enumerates the three significant national responses that have been made and are continually taken into consideration to protect the conditions of the PDL population in the face of the COVID-19 pandemic as follows:

Easing of parole grant and executive clemency rules

In May 2020, it was initially reported that 9,731 PDLs have been released. These are PDLs for offenses punishable with the incarceration of 6 months or less. Furthermore, according to the data of released PDLs in July, there were 15,102 paralegal releases through bail, a plea on deal, parole, or probation. At the same time, 6,756 PDLs were released legally after being found not guilty or having served their sentences. In August 2020, the data showed that the total number of released PDLs has increased to 58,625 [10].

However, there is another side to the argument amid the requests and reactions to release the PDLs which suggests that merely releasing them could have additional unexpected impacts on the community [14]. Employment for PDLs who have been freed is extremely difficult at any regular rate. Therefore, the conditional or final release of PDLs without support for entry into the labor market would only increase the number of unemployed people given the reported surge in the national unemployment rate brought on by the crisis.

Provision of human considerations to vulnerable groups

Another response to decongest the correctional facilities is the arrangement of the temporary release of vulnerable groups of PDLs based on humanitarian grounds. Senior citizens, PDLs with comorbidities or disabilities, and pregnant women are among the PDL-vulnerable groups who are believed to be at a high risk of contracting the virus. It also includes low-risk offenders, children in conflict with the law, and other people who are arbitrarily detained [33].

Improvement of healthcare system

Health management in correctional facilities has been improved by the combined efforts of numerous national agencies and private entities. The government has been collaborating with necessary authorities to perform "target testing" in prisons ever since it launched an extended testing program [41]. The main objective of this approach is to give PDLs access to medical care services such as preventive, curative, and palliative therapies. Additionally, the World Health Organization, Department of Health, and Committee of the Red Cross have also been collaborating closely to give technical assistance and set up quarantine facilities for afflicted PDLs [1].

Moreover, the Dangerous Drugs Board has adopted prevention policies in the admissions in drug treatment and rehabilitation facilities around the country as a measure to mitigate COVID-19 transmission. Engineering measures such as isolation corners and ventilation facilities were required because of the new constraint. Sanitation and disinfection of all locations were also introduced as crucial environmental controls. The facilities have been requested to comply with the observance of physical distancing, visitation regulations, and offer personal protective equipment.

Chapter 3

Review of Related Literature

This study is motivated by numerous research works which employed the utility of agent-based models as a platform to integrate diverse evidence sources as a support in decision-making for complex health problems caused by COVID-19. This section will provide a synthesis of findings that will support this study's results. This section will also be identifying the gaps in the results of different scientific studies administered with the same approach.

3.1 Agent-Based Modeling in COVID-19 Mitigation

A plethora of studies made findings to help the decision-making problems of policymakers amid the COVID-19 pandemic. These studies were used to inform policymakers throughout the world of the expected behavior of the COVID-19 outbreak and the proper interventions that must be administered to stem the virus from propagating at higher levels.

In a study that evaluates the nonpharmaceutical interventions including vertical and horizontal isolation, use of face masks, partial lockdowns, and social isolation, the findings suggest that lockdowns were the best-evaluated nonpharmaceutical intervention in limiting the spread of the virus and preserving lives [46].

On the other hand, one research on the COVID-19 epidemic in France inferred that while lockdown is effective in containing the viral spread, once lifted, regardless of duration, it would be unlikely to prevent a rebound. Both physical distancing and mask-wearing are effective in slowing down the epidemic and reducing mortality but would also be ineffective in ultimately preventing ICUs from becoming overwhelmed and a subsequent second lockdown [15]. This is supported by another study in India which found that prolonging the lockdown may help in the containment of the infection in the first

days however, it does not provide help if it is lifted without vaccination or having the population immune first, as this will cause the cases to shoot up again [49].

The mitigation of the spread of the infection is also simulated in various facilities including universities, school classrooms and supermarkets. In the USA, a study using an agent-based modeling approach has been developed to mimic the virus transmission dynamics in universities. Their results found that more than 99.9% of the total infections can be prevented when combined social distancing and mask use are implemented [55].

A study in the Philippines used the agent-based modeling approach to study the spread of the virus inside Philippine classrooms and infer the best classroom setup to minimize the risk of transmission. Results of the study show that the highest value of the cumulative proportion of infected individuals inside the classroom is achieved when the total allowable seating capacity in the classroom increased from 25 to 50 %. The study found that factors including the maximum number of students and the number of initially infected individuals significantly affect the likelihood apart from the seating arrangement itself [23].

Another hotspot for transmitting COVID-19 is the supermarkets. One research work studied this particular facility and found that the best intervention policy among those that were tested is to restrict the arrival rate of customers or the maximum permissible number of customers together with a mandatory face mask protocol [54].

In general, most of these studies conclude that a synthesis of proper nonpharmaceutical interventions includes the mandatory use of face masks, reduction or control of population in a given setting and lockdowns.

Chapter 4

Methodology

4.1 Model Implementation

The implemented system is a stochastic agent-based model to simulate the transmission of the COVID-19 virus inside the correctional facilities of the Philippines. The agent-based models are implemented in the GAMA Platform, an environment explicitly for agent-based modeling and simulations.

4.1.1 Simulation Space

The simulation space represents a correctional facility in a Euclidean complex network with pre-determined lower and upper limits in x axis $[L_x, U_x]$ and y axis $[L_y, U_y]$. The space is composed of prison cells $\mathbf{C}$ that are separated by 2-meter hallways. There are n number of prison cells which follows that

$$\mathbf{C} = \mathbf{C}_1, \mathbf{C}_2, \mathbf{C}_3, ..., \mathbf{C}_n$$

.

Each prison cell has its own lower and upper bounds for x and y axes namely, $[CL_x, CU_x]$ and $[CL_y, CU_y]$. For accurate measurements, the simulation space is constructed using AutoCAD, a commercial computer-aided program for 2D and 3D models. The prison cells and hallways are constructed in two different shapefiles that are integrated into the model. Figure 4.1 illustrates a representation of the simulation space.

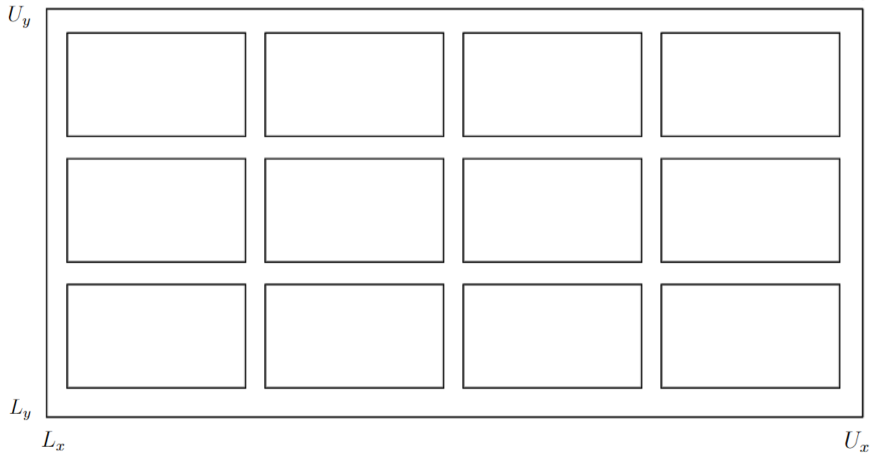

Figure 4.1: Illustration of the prison facility as the simulation space of the model with lower and upper limits of x and y axes represented by $[L_x, U_x]$ and $[L_y, U_y]$, respectively. The prison cells are separated by two-meter hallways.

4.1.2 The Agents

The prison PDLs are represented by agents that can travel and interact with one another inside the enclosed simulation space. Each agent, excluding the removed agents, has its own unique position in the *two*-dimensional simulation space (eg., if $\mathbf{s}_1$ is in (x_1, y_1) and $\mathbf{s}_2$ is in (x_2, y_2), then $x_1 \neq x_2$ and/or $y_1 \neq y_2$). In addition, each of the agent has only one possible compartmental state given by SEIRD. The states, movement rules and positions of the agents are further discussed in the next sections.

State of the Agents

The initial population $\mathbf{P}(0)$ of the agents is defined at the first iteration $t = 1$. The agents are divided into five compartments $\mathbf{S}(t)$, $\mathbf{E}(t)$, $\mathbf{I}(t)$, $\mathbf{R}(t)$, and $\mathbf{D}(t)$ which represents the total population of the susceptible, exposed, infected, recovered, and removed agents,

respectively. These follow that

$$\begin{aligned}
\mathbf{S}(t) &= \mathbf{s}_1(t), \mathbf{s}_2(t), ..., \mathbf{s}_S(t) \\
\mathbf{E}(t) &= \mathbf{e}_1(t), \mathbf{e}_2(t), ..., \mathbf{e}_E(t) \\
\mathbf{I}(t) &= \mathbf{i}_1(t), \mathbf{i}_2(t), ..., \mathbf{i}_I(t) \\
\mathbf{R}(t) &= \mathbf{r}_1(t), \mathbf{r}_2(t), ..., \mathbf{r}_R(t) \\
\mathbf{D}(t) &= \mathbf{d}_1(t), \mathbf{d}_2(t), ..., \mathbf{d}_D(t)
\end{aligned} \tag{4.1}$$

Equation 3.1 presents the number of the initial state of the model where there are no removed agents yet. For every iteration t, the number of agents from each compartment is updated. This change in number per unit time is monitored depending on the prison conditions to investigate the impact of rising congestion rates on the transmission dynamics of COVID-19. The population size may drop due to the removal of agents caused by death brought on by the disease. However, the model does not consider the removal of agents due to natural death, release by sentence expiration, or discharge due to granted parole within the simulation period. Moreover, the model does not include new admissions of PDLs during the simulation. Hence, it follows that

$$\mathbf{P}(t) = \mathbf{S}(t) + \mathbf{E}(t) + \mathbf{I}(t) + \mathbf{R}(t) = \mathbf{P}(0) - \mathbf{D}(t) \tag{4.2}$$

where $\mathbf{P}$(t) represents the current population at iteration t. The infection status of each agent can be recognized in its distinct body color as illustrated in Figure 4.2

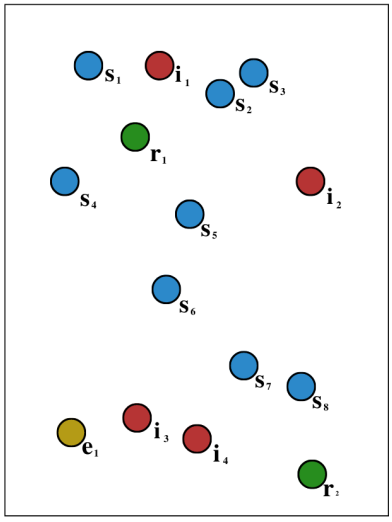

Figure 4.2: The color of the agents' bodies represents the current infection status of the agents. Susceptible, exposed, infected and recovered.

Note at the first iteration ($t = 0$), only infected and susceptible agents are in the simulation space which adheres to the following equation:

$$\mathbf{S}(t) + \mathbf{I}(t) = \mathbf{P}(0) \tag{4.3}$$

4.1.3 Movement of Agents

The movement of the agent can be achieved by adding a random numerical value to the original coordinates of the agents. The random numerical value is within $[-L, L]$ where L represents the maximal permissible perturbation. The value of L corresponds to the movement performed by the individuals when they interact within the simulation space. These movements are emulated under the following formulation

$$\begin{aligned} x_{t+1} &= x_t + \text{rnd}(-1, 1) \cdot L \\ y_{t+1} &= y_t + \text{rnd}(-1, 1) \cdot L \end{aligned} \tag{4.4}$$

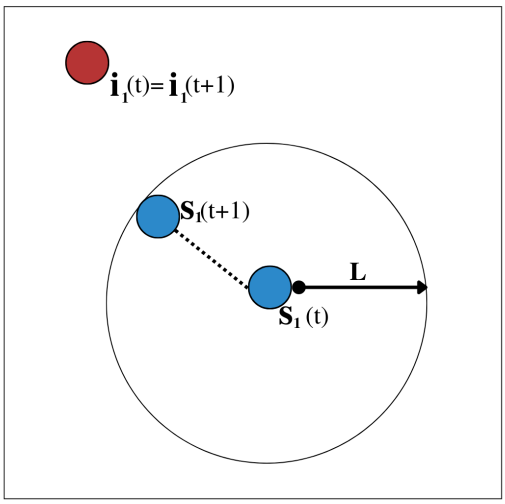

Figure 4.3: Operation for movement rule. The infected agent $\mathbf{i}_1$ remained at its position while the susceptible agent $\mathbf{s}_1$ changed its position within the maximal permissible perturbation L.

4.1.4 Initialization

Each experiment starts with iteration ($t = 0$) where the model loads and sets the required variables for the simulations. In this process, the model loads the shapefiles into the simulation to serve as the two-dimensional space for the agents to move at. Note that only susceptible and infected agents are present in the first iteration of the simulation.

Assigning the infection state

At the first iteration ($t = 0$), the model assigns the infection status of each agent. The number of initially infected agents I is pre-specified. Using this, the model randomly selects agents and assigns them as infected $\mathbf{I}(0) = \mathbf{i}_1(0), \mathbf{i}_2(0), ..., \mathbf{i}_I(0)$. Otherwise, if the agent is not assigned infected, it will automatically be susceptible $\mathbf{S}(0) = \mathbf{s}_1(0), \mathbf{s}_2(0), ..., \mathbf{s}_S(0)$.

Assigning of prison cells and position

The initialization includes randomly assigning each of the PDLs in the initial population $\mathbf{P}(1)$ to one of the available prison cells $\mathbf{C} = \mathbf{C}_1, \mathbf{C}_2, \mathbf{C}_3, ..., \mathbf{C}_n$. For example, $\mathbf{i}_1$, $\mathbf{s}_1$, and $\mathbf{s}_2$ are assigned in $\mathbf{C}_1$ while $\mathbf{s}_3$, $\mathbf{s}_4$, and $\mathbf{s}_5$ are assigned in $\mathbf{C}_2$, as seen in Figure 4.4

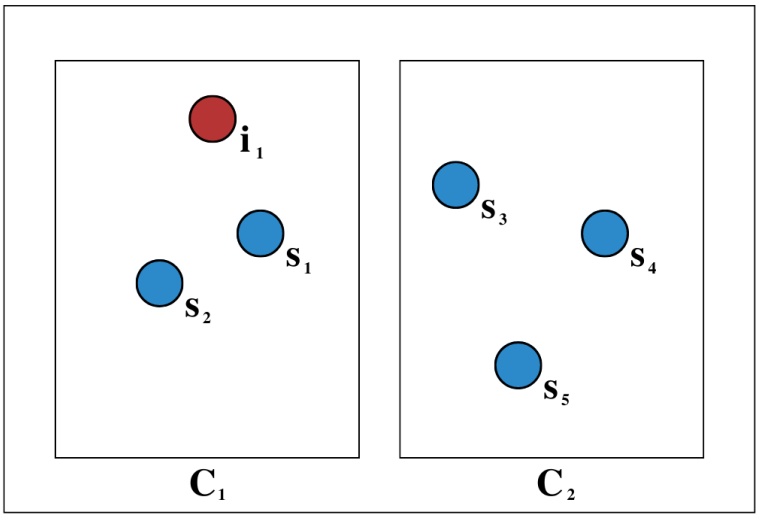

Figure 4.4: An illustration of the rule for assigning prison cell for agents

Subsequently, the model starts generating the positions of each agent from $\mathbf{S}(t)$ and $\mathbf{I}(t)$ inside its assigned prison cell. In this process, each coordinate of $\mathbf{s}_n$ and $\mathbf{i}_m$ ($n \in 1, 2, ..., S; m \in 1, 2, ..., I$) is set with a numerical value uniformly determined between the defined lower and upper limits of x and y of its assigned prison cell given by $[CL_x, CU_x]$ and $[CL_y, CU_y]$, respectively so that the x and y coordinates are

$$\begin{aligned} x &= CL_x + \text{rnd}(0,1) \cdot (CU_x - CL_x) \\ y &= CL_y + \text{rnd}(0,1) \cdot (CU_y - CL_y) \end{aligned} \tag{4.5}$$

where $\text{rnd}(0,1)$ is a function that generates a random positive real number within a uniform distribution $\boldsymbol{U}[0,1]$.

Movement status

In the model, some of the agents can move along the hallways while some are restricted and can only move inside their assigned prison cell. The number of agents that can move along the hallways $\mathbf{P}_{wander}$ are pre-determined. At the start of the simulation, the model randomly assigns agents who can move along the hallways based on the value of $\mathbf{P}_{wander}$. If the agent is permitted to wander outside its assigned prison cell, it can wander throughout the simulation with set bounds as $[L_x, U_x]$ and $[L_y, U_y]$. On the other hand, if the agent is not authorized to wander outside its assigned prison cell, the model sets the bounds of its permitted wandering positions to its assigned prison cell $[CL_x, CU_x]$ and $[CL_y, CU_y]$ using the integrated shapefile.

4.1.5 Exposure Rule

For each of the infected agents, the model examines the existence of any susceptible agent in the pre-specified neighborhood with a radius n. For this model, n is assigned to be 2 meters, which supports the current 2-meter safe distance recommendation between two people [3]. If the model confirms the existence of susceptible PDLs around the infected ones, the susceptible PDLs will automatically be classified as exposed. In this process, the model calculates the distance of the newly exposed PDL to the infected one and stores it in parameter d. This distance d will be used in the infection rule that will be discussed in the next section.

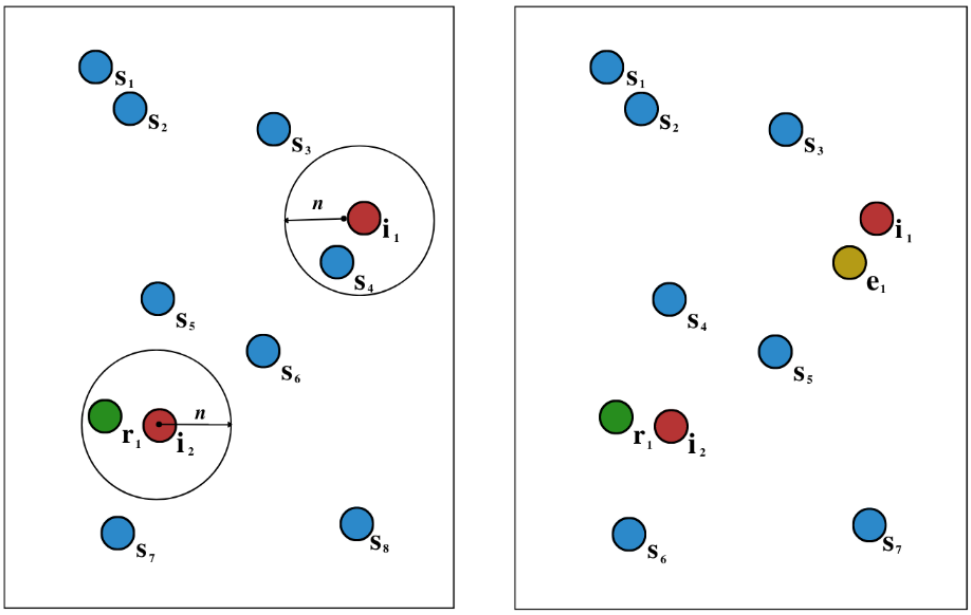

(a) Initial configuration at time (t) (b) Final configuration at time $(t+1)$

Figure 4.5: Operation for the exposure rule. The initial configuration 4.5(a) presents two agents $\mathbf{s}_4$ and $\mathbf{r}_1$ that are within the neighborhood of the infected agents $\mathbf{i}_1$ and $\mathbf{i}_2$, respectively. In the next configuration $(t+1)$ in 4.5(b), $\mathbf{s}_4$ changed into an exposed state as $\mathbf{e}_1$ while $\mathbf{r}_1$ stayed in its recovered state.

Figure 4.5 illustrates the operation process in the exposure rule. Assume that Figure 4.5 (a) exhibits the simulation status at time t and Figure 4.5 (b) shows the status of the same simulation at time $(t+1)$. In the figure, it considered a set of 8 susceptible PDLs, 2 infected and 1 recovered PDL $[\mathbf{S}(t) = 8, \mathbf{E}(t) = 0, \mathbf{I}(t) = 2, \mathbf{R}(t) = 0, \mathbf{D}(t) = 0]$ with a total population of 11 agents $(\mathbf{P}(t) = 11)$. The figure clearly shows that PDLs s_4 and r_1 are within the neighborhood of infected agents i_1 and i_2, respectively. At the next iteration $(t+1)$, the susceptible agent s_4 became an exposed agent e_1 while the recovered or immune agent r_1 maintains its compartment status, despite the contact with an infectious individual.

When a susceptible PDL becomes exposed at day t, the model assigns the number of days for which the exposed individual will be incubated INC_L. The exposed phase or incubation period INC_L is used to describe the period of time between exposure to

the virus and the time the disease becomes apparent through symptoms and signs. The mean incubation time for COVID-19 ranged from 5.6 to 6.7 days [37]. This model uses 6 days as a constant incubation period for each exposed PDL. On the 6th day of the incubation period $(t + 6)$, the agent can be infected or will be back to its susceptible state.

4.1.6 Infection Rule

When an exposed PDL finishes its incubation period INC_L, the model will probabilistically decide if the exposed PDL will continue to be infectious or if it will be back to a susceptible state, which means that the PDL is not infected despite the recent contact with an infected PDL. Given the distance to the infected PDL d, which was generated during the exposure period, the model generates the probability that the exposed agent will be infected PRI. To compute this, the model uses the probability of infection function that was generated in one study as given in Figure 4.6.

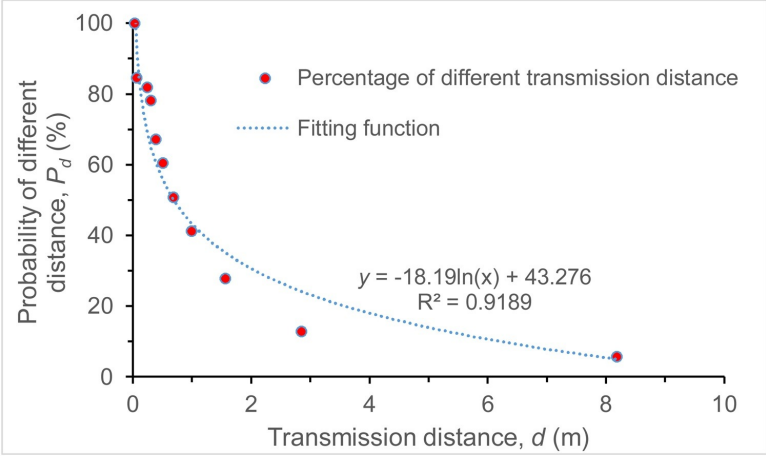

Figure 4.6: The relationship between droplet transmission distance and the probability of COVID-19 infection [48]

The probability of infection function is a function with respect to the distance of the exposed agent to the infected one. In this process, the model uses the value of d, which was generated during the exposure time as the variable of the function. The function is given by

$$PRI = \frac{-18.19 \ln(d) + 43.276}{100} \tag{4.6}$$

Note that the function only takes into consideration that COVID-19 is an airborne disease. Hence, fomite transmission and other indirect contact are not incorporated in the given probability of infection PRI. It can be shown that the probability of infection of an exposed individual strongly reduces relative to its distance from an infected agent.

After generating the probability of infection PRI for the exposed agent, the model generates a random positive real number r within a uniform distribution $\mathbf{U}[0, 1]$. If the value of the generated random number r is greater than the generated value of PRI, the exposed PDL is considered to be infected, otherwise, it will return to its susceptible state.

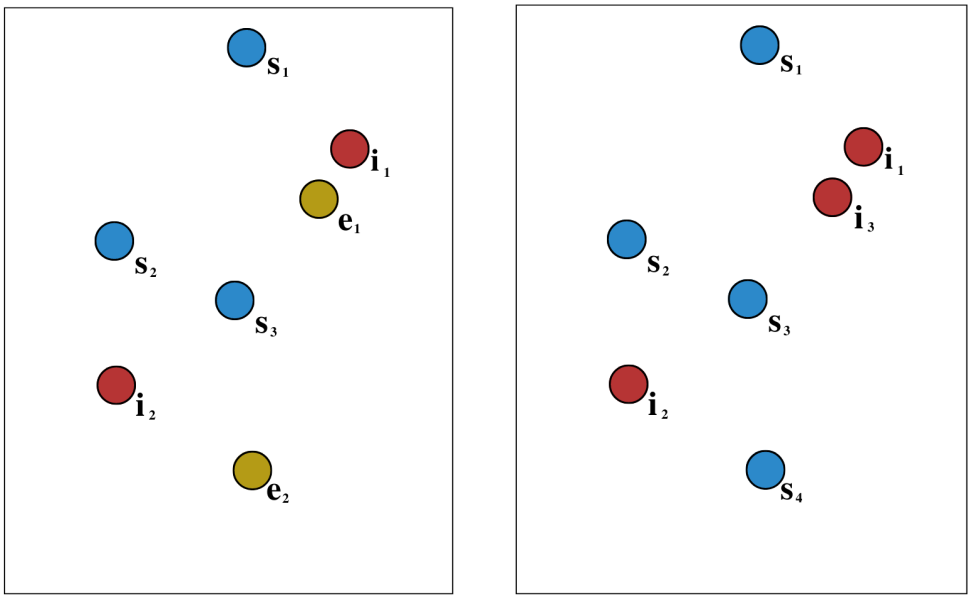

(a) Initial configuration at time (t) (b) Final configuration at time $(t+1)$

Figure 4.7: Operation for the infection rule. The initial configurations show two individuals in an exposed state, $\mathbf{e}_1$ and $\mathbf{e}_2$ at time t. The final configurations illustrates that $\mathbf{e}_1$ changed to an infected state $\mathbf{i}_2$ while $\mathbf{e}_2$ was back to its susceptible state $\mathbf{s}_4$ at $(t+1)$.

Figure 4.7 illustrates the process of the infection rule. Figure 4.7(a) presents the initial configuration which has 7 total agents in which 3 are susceptible ($\mathbf{S}(t) = \mathbf{s}_1, \mathbf{s}_2, \mathbf{s}_3$), 2 are

infected ($\mathbf{I}(t) = \mathbf{i}_1, \mathbf{i}_2$) and 2 are exposed ($\mathbf{E}(k) = \mathbf{e}_1, \mathbf{e}_2$). The variable d for $\mathbf{e}_1$ and $\mathbf{e}_2$ are given in Table 4.1. It can be seen that d of $\mathbf{e}_1$ is lower than of $\mathbf{e}_2$ which indicates that $\mathbf{e}_1$ is closer to an infected agent than $\mathbf{e}_2$ when they were exposed to an infected agent. The generated probabilities of infection for both agents in exposed states are also given in the table. Assume that the model generates identical random numbers for both exposed agents then $\mathbf{e}_1$ will become infected while $\mathbf{e}_2$ will not. The final configuration in Figure 4.7(b) clearly demonstrates that $\mathbf{e}_1$ became infected while $\mathbf{e}_2$ is back to its susceptible state.

Agent	d	PRI	r	Outcome
$\mathbf{e}_1$	0.2m	0.72 %	0.50	not infected
$\mathbf{e}_2$	1.5m	0.72 %	0.50	infected

Table 4.1: Table of values for the example scenario for infection rule

When an exposed agent becomes infected at day t, the model assigns the number of days for which the infected individual will be infectious INF_L. The mean infectious duration for symptomatic cases is 13.4 days while the potential maximum infectious duration is 18.1 days [9] thus this model sets the minimum and maximum infection duration to 13 and 18 days, respectively ($INF_{min} = 13$ and $INF_{max} = 18$). After the infectious period ($t+INF_L$), the agent can recover from the disease and will be considered immune for a certain amount of time, or it can also be removed from the population due to death. This process will be intensively discussed in the next section.

4.1.7 Recovery or Deceased Rule

The model evaluates all infected agents who have finished their infectious period. The outcome of the infection will be determined by stochastically deciding if the infected PDL will recover and become immune to the COVID-19 virus or if it will expire and be removed from the simulation space. The death rate is given by δ which is equal to the constant 0.0224. The value of δ is taken from the death rate inside the Philippine prisons in 2020. The model will generate a random positive real number from the uniform distribution $\mathbf{U}[0, 1]$. If the generated r is greater than the value of δ, the agent will recover

and be immune from the disease for N number of days, otherwise, it will be deceased and removed from the population. This model sets N to 100 days [40].

4.1.8 Adherence of Nonpharmaceutical Interventions

The following sections discuss the procedure for the implementation of nonpharmaceutical interventions which are considered in this study to evaluate its impact. The values of variables and parameters will also be elaborated.

With mandatory face masks

To compare the simulated effects of the mandatory use of the face mask intervention strategy, the model quantifies the strategy's effect on the extent of transmissibility between individuals. For example, assume that using face masks can reduce the probability of infection PRI for the agent in the exposed state to be infected by λ percent. Then, the expected probability of infection will be recomputed with the following formulation

$$PRI_{new} = PRI - (PRI \cdot \lambda) \tag{4.7}$$

This means that the value of the new probability of infection PRI_{new} is less than λ percent of its original value PRI. For this study, the model sets the value λ to 0.47, indicating that using a face mask can reduce the probability of infection by 47% [26]. To demonstrate this process, consider that the initially generated probability of infection for an agent is 0.46 ($PRI = 0.46$). Assume that this agent is following the mandatory use of face mask protocol properly, then its new probability of infection can be computed as follows

$$\begin{aligned} PRI_{new} &= PRI - (PRI \cdot \lambda) \\ &= 0.46 - (0.46 \cdot 0.47) \\ &= 0.2438 \end{aligned} \tag{4.8}$$

The use of face masks strongly reduced the probability that the agent in an exposed state will be infected.

With mobility restrictions

The mobility restrictions will be implemented using the discussed movement rule in the previous section. The model considers different percentages of individuals who can wander along the hallways.

4.2 Computational Procedure

In this section, the constant parameters and variables used in the implementation of the model including the computation of rates to generate the results of the study will be reviewed.

4.2.1 Main Parameters of the Model

The following table provides the summary of the constant parameters which will be used in the model.

Parameter	**Value/range of value**	**Reference**
Incubation duration INC_L	6 days	[37]
Infection duration INC_L	[13-18] days	[9]
Fatality rate δ	0.0224	[A]
Immunity duration	100 days	[40]
λ	0.47	[26]
Permissible Perturbation L	1.0m	Author's estimation

Table 4.2: Summary of constant parameters used in the agent-based model.

The simulation space that represents a specific correctional facility is a Euclidean complex network with a lower and upper bound for x and y axes, $[L_x, U_x]$ and $[L_y, U_y]$. These are altered depending on the different experimental conditions and cases to simulate. The following data about the area of the seven correctional facilities were provided by the Bureau of Corrections. This study sets $L_x = L_y = 0$, thus it follows that

Correctional Facility	**Total Floor Area**	U_x	U_y
New Bilibid Prison	37807.72 sq.m	137.49	274.98
Correctional Institute for Women	5920.00 sq.m.	54.41	108.81
Iwahig Prison and Penal Farm	3066.00 sq.m.	39.15	78.31
Davao Prison and Penal Farm	8279.00 sq.m.	64.34	128.68
San Ramon Prison and Penal Farm	4309.00 sq.m.	46.42	92.83
Sablayan Prison and Penal Farm	5841.00 sq.m.	54.04	108.09
Leyte Regional Prison	3991.00 sq.m.	44.68	89.35

Table 4.3: Table for the total floor area, and upper bounds (U_x, U_y) of the Philippine correctional facilities A

4.2.2 Rates

At each time t, the changes in the population in each compartment are monitored. Let β represent the exposure rate, α represent the infection rate, γ is the recovery rate, and δ signifies the death rate. Each rate of these compartments over time is computed as follows

$$\begin{aligned} \beta(t) &= \frac{\mathbf{E}(t)}{\mathbf{P}(0)} \\ \alpha(t) &= \frac{\mathbf{I}(t)}{\mathbf{P}(0)} \\ \gamma(t) &= \frac{\mathbf{R}(t)}{\mathbf{P}(0)} \\ \delta(t) &= \frac{\mathbf{D}(t)}{\mathbf{P}(0)} \end{aligned} \tag{4.9}$$

where E, I, R, D and $\mathbf{P}(0)$ represent the number of exposed, infected, recovered, expired and initial population of agents, respectively.

4.2.3 Percentage of the exposed population who will contract the disease

This study needs to evaluate the percentage of individuals who are in an exposed state and will not be infected despite the contact. The result of this process helps in the generation of inferences on the effect of nonpharmaceutical interventions on the evolution of the disease, specifically for the mandatory use of face masks.

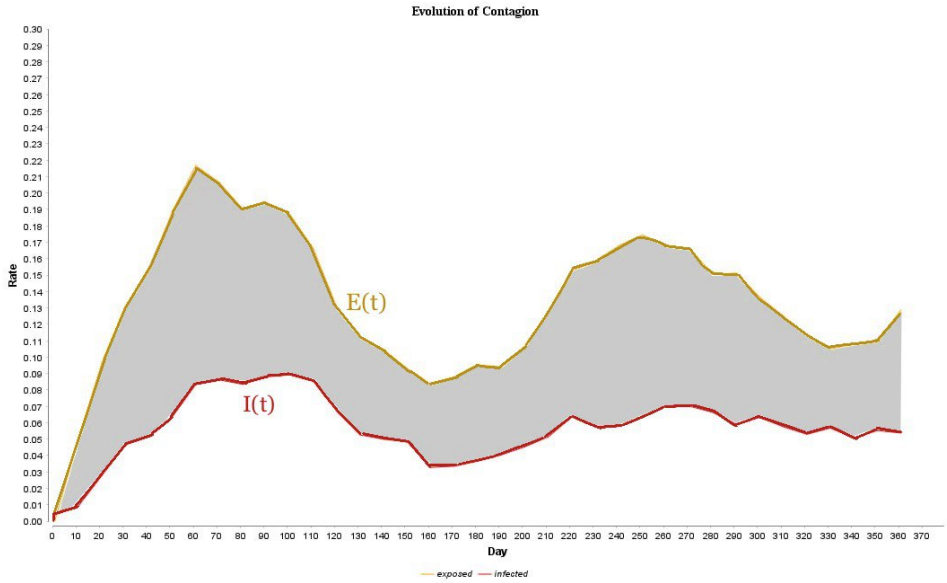

Figure 4.8: The graph for the functions of exposure rate $E(t)$ and infection rate $I(t)$. The shaded area represents the percentage of individuals who are exposed to an infected agent but did not contract the disease despite the contact.

Let A represent the percentage for which the exposed population will contract the disease. Further, suppose that $E(t)$ is the function of the exposure rate with respect to time t and $I(t)$ represents the infection rate over time t. In Figure 4.8, the exposure rate is relatively higher than the infection rate. This infers that not all individuals who are in an exposed state will eventually be infected. The shaded area between the functions $E(t)$ and $I(t)$ represents the percentage of individuals who are exposed to the virus but were not infected. This percentage can be computed by getting the area under the curve of the function $E(t)$ and subtracting this from the area under the curve of the function

$I(t)$. Thus, the computation can be done as follows

$$A = \int_1^{365} E(t)dt - \int_1^{365} I(t)dt \tag{4.10}$$

4.3 Gathering of Data

The data on the PDL population, floor area, capacity and congestion rates were provided by the Philippine Bureau of Corrections through appeals from the Freedom of Information Philippines website. The data were provided upon the requests of the author.

Supplementary data regarding the standard Philippine prison building specifications are retrieved from the Official Gazette of the Republic of the Philippines website. This website is the official journal of the Republic of the Philippines, an online version of the print edition of the Official Gazette, which was created by decree of Act No. 453 and Commonwealth Act No. 638.

Chapter 5

Results and Discussion

In this section of the study, the effects of high occupancy rates in Philippine prisons are first simulated. Then, three control strategies including the use of face masks, lockdown measures and limiting PDL activity are designed and implemented in the model to simulate the effect of each.

Each time cycle in the simulation represents one day and the time span for the simulations is one year. Hence, each simulation runs for 365 iterations, representing the days in a year. The number of simulation runs for an PDL-based model that is necessary to provide enough validation and confidence that the calculated statistics can represent the distribution of the model samples is determined to be 30 runs [16]. Thus, chosen simulated scenarios in this model are run 30 times with the same variable. One graph for each simulated experiment is presented to provide clear visualization of the results.

5.1 Effect of High Congestion Rates to COVID-19 Outbreak

To study the effect of the high congestion rates, the model simulates the transmission of COVID-19 infection without any health protocol. The variables that will be used in the next simulations are only the initial population $\mathbf{P}(0)$ and the lower and upper bounds of x and y axes to represent the total area of the facility.

Correctional Facility	$\mathbf{P}(0)$ for ideal capacity	$\mathbf{P}(0)$ for actual capacity
New Bilibid Prison	6435	28456
Correctional Institute for Women	1008	3311
Iwahig Prison and Penal Farm	675	2739
Davao Prison and Penal Farm	1357	6408
San Ramon Prison and Penal Farm	733	2208
Sablayan Prison and Penal Farm	994	2573
Leyte Regional Prison	679	2025

Table 5.1: Table presenting the total population $\mathbf{P}(0)$ when the facility is at its ideal capacity and $\mathbf{P}(0)$ when the facility is at its actual occupancy rate in 2020. A

Table 5.1 presents the initial population that will be considered to simulate the scenarios with different congestion rates. The model assumes there are no nonpharmaceutical interventions that are administered thus, the PDLs are not wearing face masks and are unrestricted in their movement in the facility. Both simulations generated for each correctional facility use the same variables and parameters except at $\mathbf{P}(0)$.

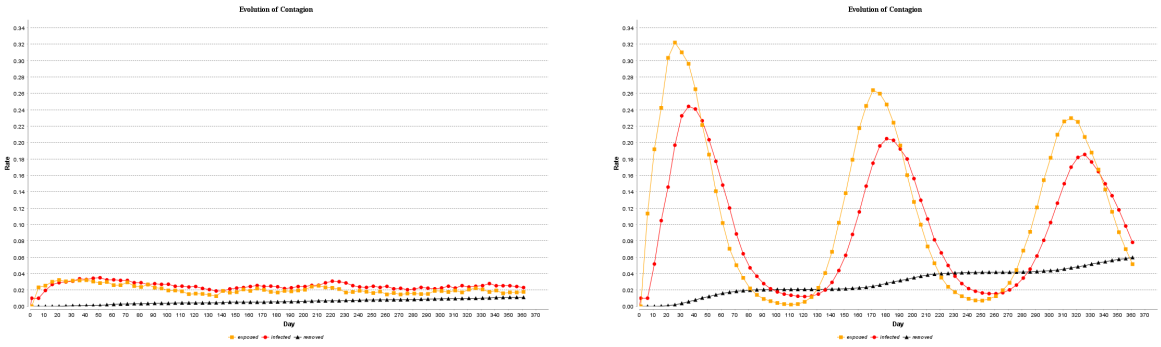

(a) $\mathbf{P}(0)$ is at facility's recommended maximum capacity

(b) $\mathbf{P}(0)$ is at its 2020 occupancy rate

Figure 5.1: Plots showing exposed, infected and removed curves in New Bilibid Prison under no protocols.

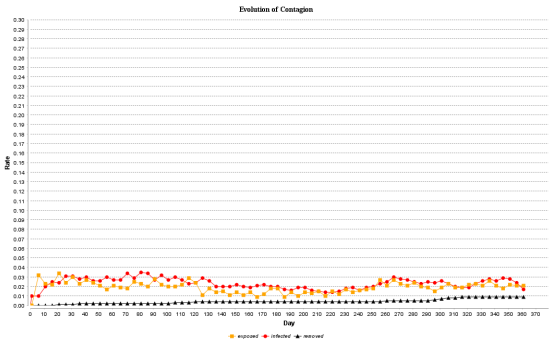

(a) $\mathbf{P}(0)$ is at facility's recommended maximum capacity

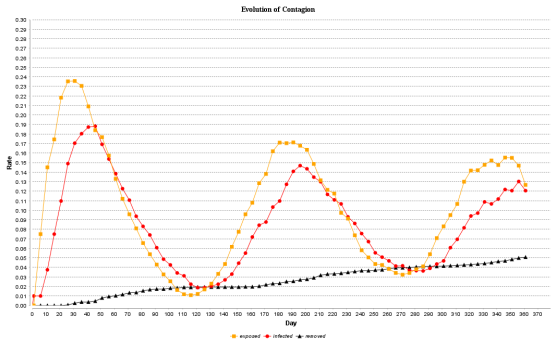

(b) $\mathbf{P}(0)$ is at facility's 2020 occupancy rate

Figure 5.2: Plots showing exposed, infected and removed curves in Correctional Institute for Women - Mandaluyong under no protocols.

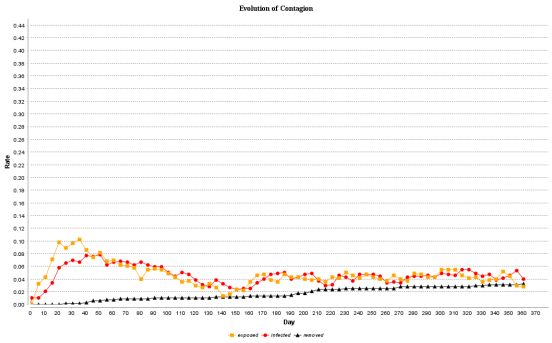

(a) $\mathbf{P}(0)$ is at facility's recommended maximum capacity

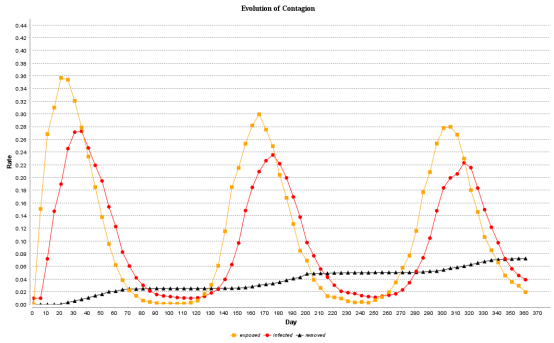

(b) $\mathbf{P}(0)$ is at facility's 2020 occupancy rate

Figure 5.3: Plots showing exposed, infected and removed curves in Iwahig Prison and Penal Farm under no protocols.

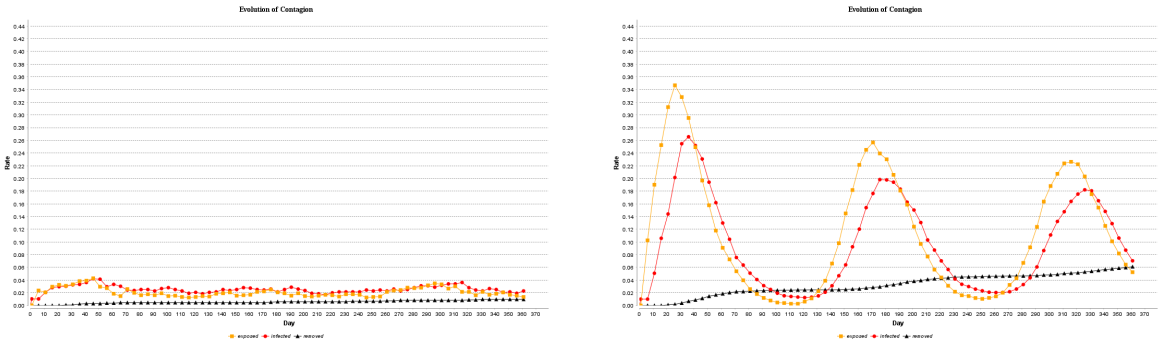

(a) $\mathbf{P}(0)$ is at facility's recommended maximum capacity

(b) $\mathbf{P}(0)$ is at facility's 2020 occupancy rate

Figure 5.4: Plots showing exposed, infected and removed curves in Davao Prison and Penal Farm under no protocols.

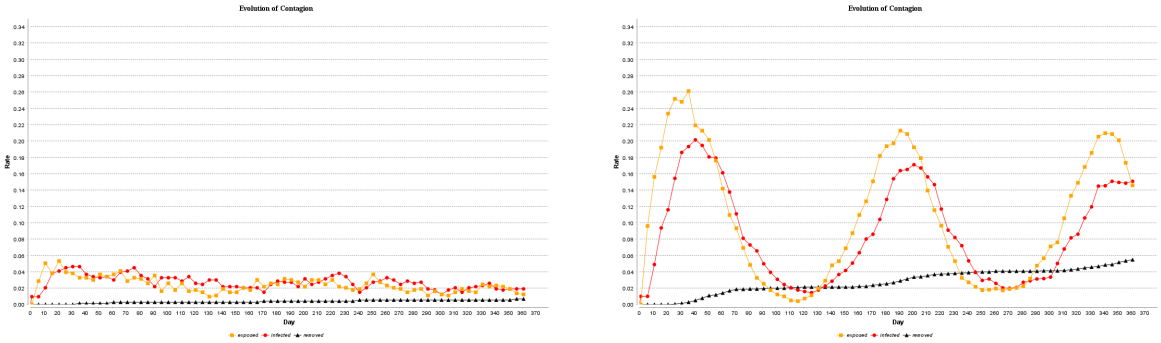

(a) $\mathbf{P}(0)$ is at facility's recommended maximum capacity

(b) $\mathbf{P}(0)$ is at facility's 2020 occupancy rate

Figure 5.5: Plots showing exposed, infected and removed curves in San Ramon Prison and Penal Farm under no protocols.

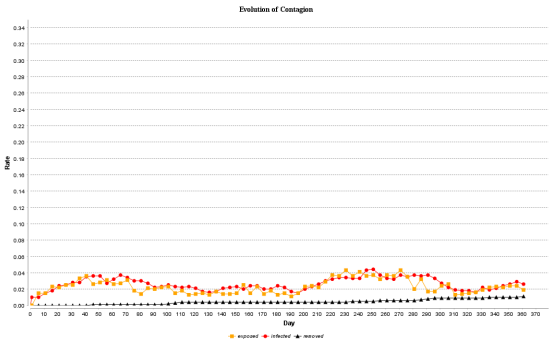

(a) $\mathbf{P}(0)$ is at facility's recommended maximum capacity

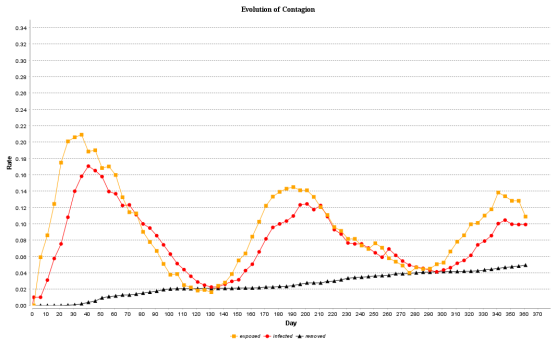

(b) $\mathbf{P}(0)$ is at facility's 2020 occupancy rate

Figure 5.6: Plots showing exposed, infected and removed curves in Sablayan Prison and Penal Farm under no protocols.

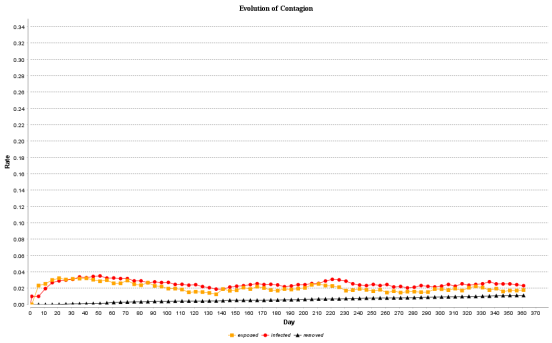

(a) $\mathbf{P}(0)$ is at facility's recommended maximum capacity

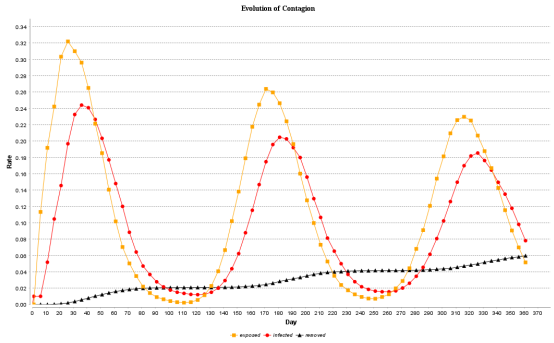

(b) $\mathbf{P}(0)$ is at facility's 2020 occupancy rate

Figure 5.7: Plots showing exposed, infected and removed curves in Leyte Regional Prison under no protocols.

The above figures clearly illustrate the difference in the evolution of the contagion of COVID-19 infection inside the seven correctional facilities. When $\mathbf{P}(0)$ is following the facility's recommended capacity, the epidemic curve shows a plateau with a rapid rise from day 19 to day 41 of the simulation. The rise is followed by a gradual decline and subsequently stabilizes with lower rates in the succeeding days. The infection cases are spread over a greater period of time. The plateau curve suggested that the PDLs are not

rapidly infected due to lower chances of contact with infected individuals. The highest average rate recorded ranges from 3.47% to 8.48%.

On the other hand, when $\mathbf{P}(0)$ is at the facility's actual occupancy rate in 2020, the epidemic curve shows a propagated curve with taller peaks and repeated waves. For all the facilities, the number of infected cases fluctuated in the first month until it reaches its apex on days 38 to day 45. This is immediately followed by a rapid decline and another wave with lower peaks. The highest recorded infection rate ranges from 17.21% to 27.38%, which is at most 23.91% higher than when the facility is following its recommended capacity.

5.2 Experiments on Nonpharmaceutical Interventions

To evaluate the effects of the nonpharmaceutical health strategies that can be implemented, this study runs simulations in different scenarios. The following model considers the average congestion rate in 2020 to set the value for $\mathbf{P}(0)$. The average congestion rate in all correctional facilities under the Bureau of Corrections is 258.14%. The experiments will use the San Ramon Prison and Penal Farm as the simulation space. Table 5.2 summarizes the parameters which will be used in each experiment in the subsequent subsections.

Parameters	**Values**
Congestion rate	258.14%
Occupancy rate	358.29 %
Initial Population $\mathbf{P}(0)$	2626
Recommended capacity	733
Total floor area	4309.0 sq.m.
$[L_x, U_x]$	$[0.0, 46.42]$
$[L_y, U_y]$	$[0.0, 92.83]$

Table 5.2: Summary of the parameters that are used in the experiments.

5.2.1 Baseline

The following established baseline PDL-based model replicates a scenario that will be used for comparison of the impact of nonpharmaceutical methods that will be simulated in subsequent experiments. There are no established protocols in the following simulation that will alleviate the virus. The PDLs are unrestricted in their movement throughout the specified simulation space.

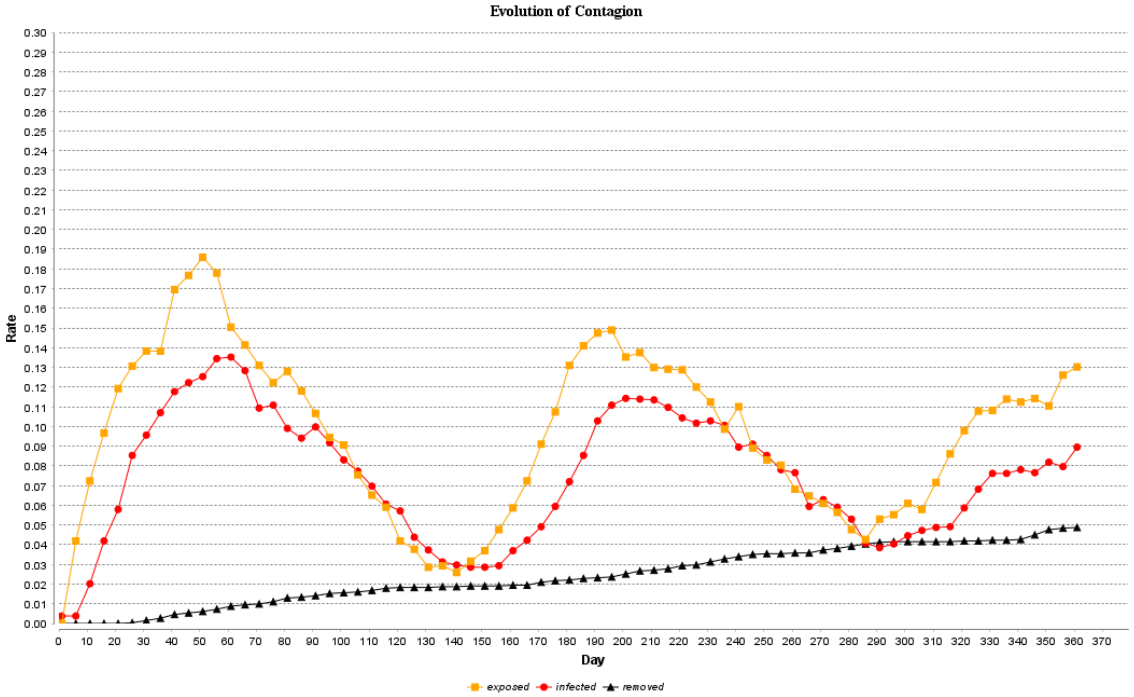

Figure 5.8: Plot Showing the Exposed, Infected and Removed Curves for Philippine Correctional Facility Under No Protocols

When there are no nonpharmaceutical interventions in place, the 30 simulations run [B] found that the average infection rate peak is 15.05% with a standard deviation of 1.99. From the simulations, the infection rate peaks between day 41 to day 76. This indicates that the first outbreak of the virus is expected in the first quarter of the year. Moreover, it was analyzed from the simulations that an average of 73% of the exposed individuals throughout the simulation were infected.

Figure 5.8 is taken from one of the 30 simulations. From the epidemic curve, it can be seen that there is a sharp increase in the number of positive cases from the first day,

indicating a high transmission within the simulation space since there are no restrictions on the interactions of the PDLs. The curve peaked on day 59 and eventually decreases until day 151 and was followed by a secondary wave with a lower infection rate peak. The second wave lasted for 139 days which was followed by another wave. The decrease in infection rates is caused by the immunity of the PDLs from the disease due to recent infection. However, the PDLs will eventually be back to being susceptible and would most likely be infected again, causing the subsequent wave in the epidemic curve. The successive waves tend to involve more PDLs until the pool of susceptible individuals is exhausted. Repeated peaks on the epidemic curve are to be anticipated until a health protocol is administered.

5.2.2 Mandatory Use of Face Masks

This experiment assumes that all PDLs are properly following the use of face mask protocol. To see the extent of the impact of the intervention, there are no mobility restrictions that are yet to be implemented.

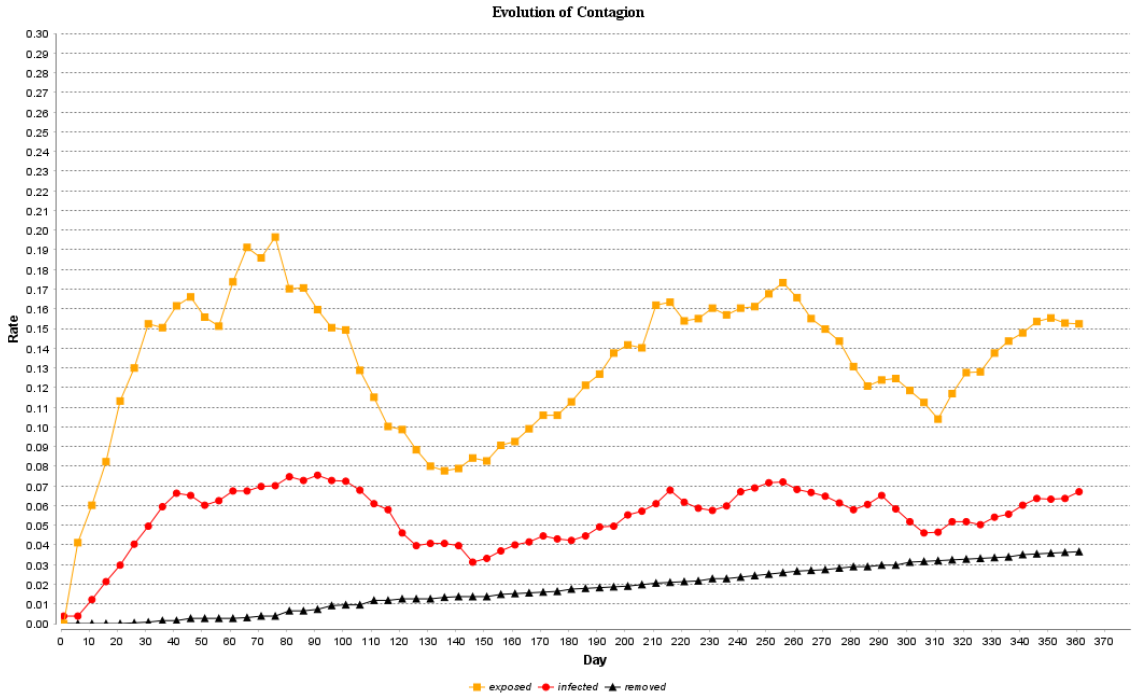

Figure 5.9: Plot showing the exposed, infected and removed curves for Philippine correctional facility under mandatory use of face mask protocol

The results from the 30 simulation run [C] found that the average highest infection rate is 9.13% with a standard deviation of 1.01, indicating a significant 5.92% decrease from the experiment when no protocols are implemented. The simulations listed that the epidemic peaks are from day 59 to day 107. This signifies that the growth of new infection cases is gradual. Despite the unrestricted interactions of the PDLs within the simulation space, the infection progresses slower. Thus, having a face mask can reduce the chance of getting infected by 39.33%.

The epidemic curve in Figure 5.9 shows the evolution of contagion from one of the executed simulations for this experiment. Notice that the first wave in the exposure rate curve resembles the curve from the baseline model however, the waves of the infection curve are not as elevated as the waves when there is no protocol that has taken place. The exposure rate in the graph reached its highest point on day 79 at 19.8% though, on the next day, the infection curve peaked at only 7.6% infection rate. This means that even though the same amount of individuals are being exposed to the virus, fewer individuals

are being infected. This is supported by the results of the 30 simulations which revealed that only 30.7% of the exposed individuals became infected which is 42.3% lower than on the baseline model. ‘

5.2.3 Mobility Restrictions

To evaluate the impact of mobility restrictions on the propagation of the COVID-19 disease, this study considers different scenarios to simulate. The different levels of intensity of lockdowns, the timing of the first execution of the mobility measures, and the lowering of chances of human mobility will be considered in the next experiments.

Level of Intensity of Lockdowns

The model considers different intensities of lockdown measures to magnify the impact of the lockdown policy on stanching the increase in the number of cases. For the following experiments, it will be considered that all individuals are properly using face masks throughout the simulation. The following figures show the evolution of propagation of the infection at different values of P_{wander}, or the percentage of the population who are allowed to move along the hallways throughout the simulation.

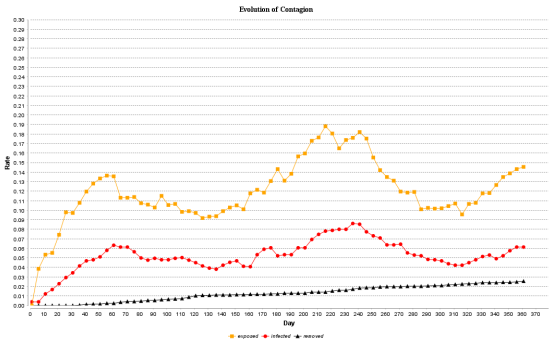

(a) 100%

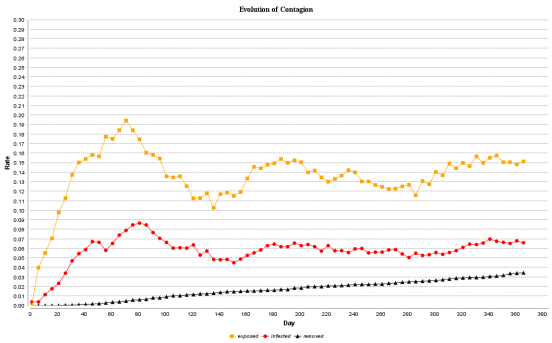

(b) 90%

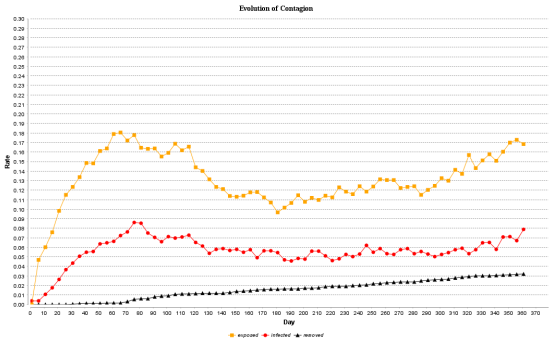

(c) 80%

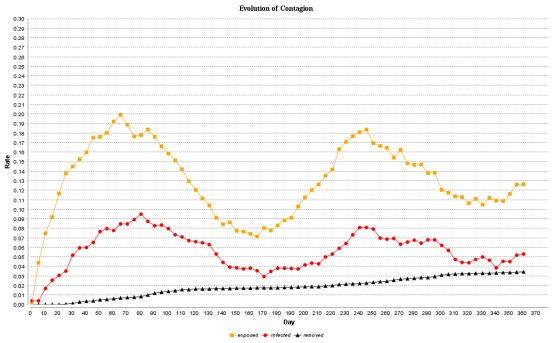

(d) 70%

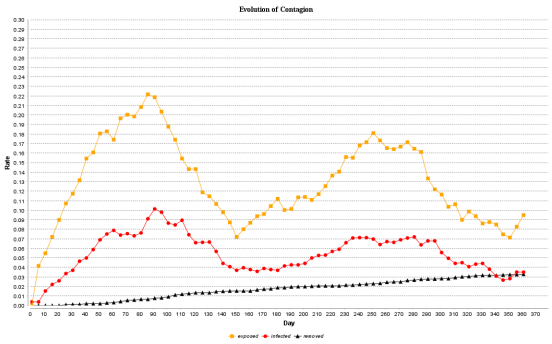

(e) 60%

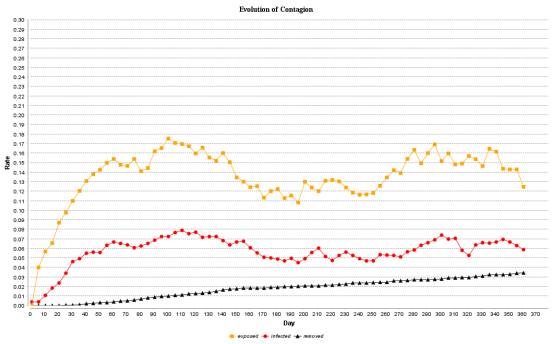

(f) 50%

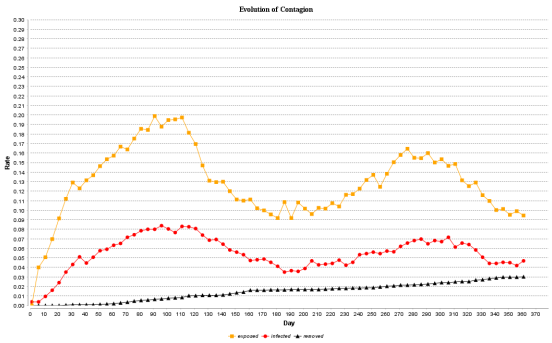

(g) 40%

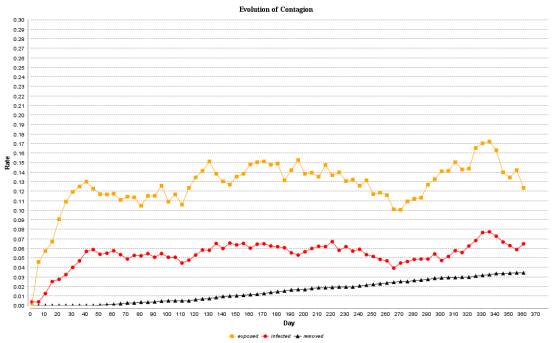

(h) 30%

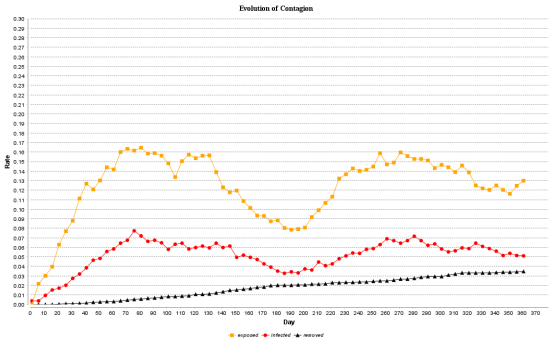

(i) 20%

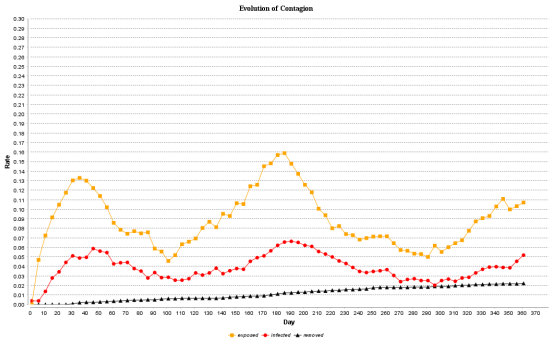

(j) 10%

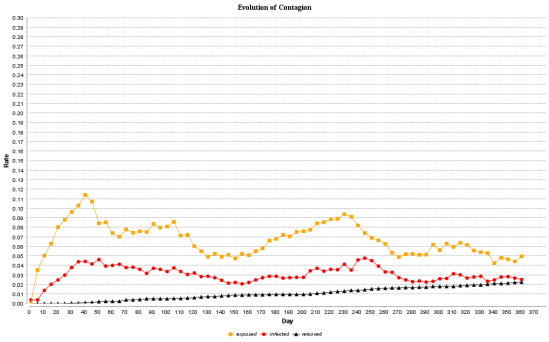

(k) 5%

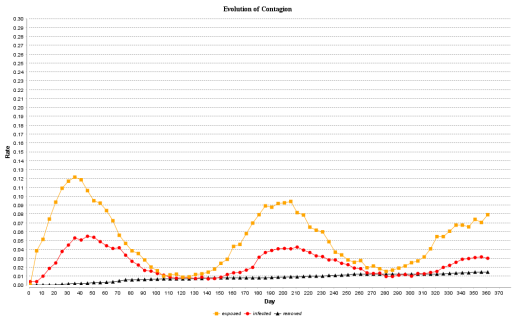

(l) Total Lockdown

Figure 5.9: The evolution of contagion of the COVID-19 infection inside Philippine prisons under different levels of lockdown intensities.

The average highest recorded infection rate when there are no mobility restrictions implemented is found to be 9.13%. Figure 5.10(a) illustrates the graph of this simulation. In the figure, the infection curve has multiple waves but the second wave has a higher

infection rate peak. The succeeding graphs appear to have multiple waves with some having a more flattened curve. See that as the value of P_{wander} decreases, the infection rates relatively decrease. This infers that a less strict policy on lockdowns would allow the transmission and would not contribute to the decrease of the infection rates.

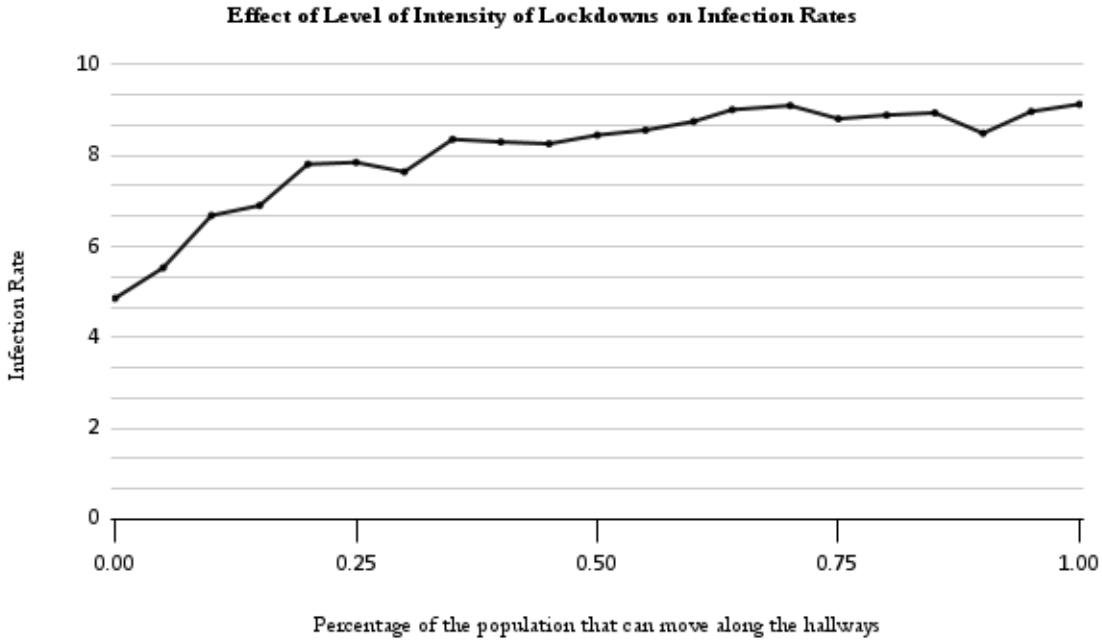

Figure 5.10: Plot showing the effect of increasing level of lockdown intensities on the infection rate peaks of COVID-19 infection.

Figure 5.10 presents the COVID-19 infection rates inside Philippine correctional facilities at different levels of lockdown intensity. At total lockdown, the highest infection rate is listed at 4.76%. From this, the infection rate rapidly increased and almost doubled until the scenario from which 25% of the population can move along the hallways. From $P_{wander} = 0.25$ until $P_{wander} = 1.0$, the maximum infection rate values steadily increased. This indicates an insignificant impact of these lockdowns on the intensities of stemming the propagation of the virus. This study thus infers that lockdown policies can only be significant in the stanch of the infection spread when there is a total lockdown or at most 5% of the population are allowed to move along the hallways for a short and scheduled amount of time.

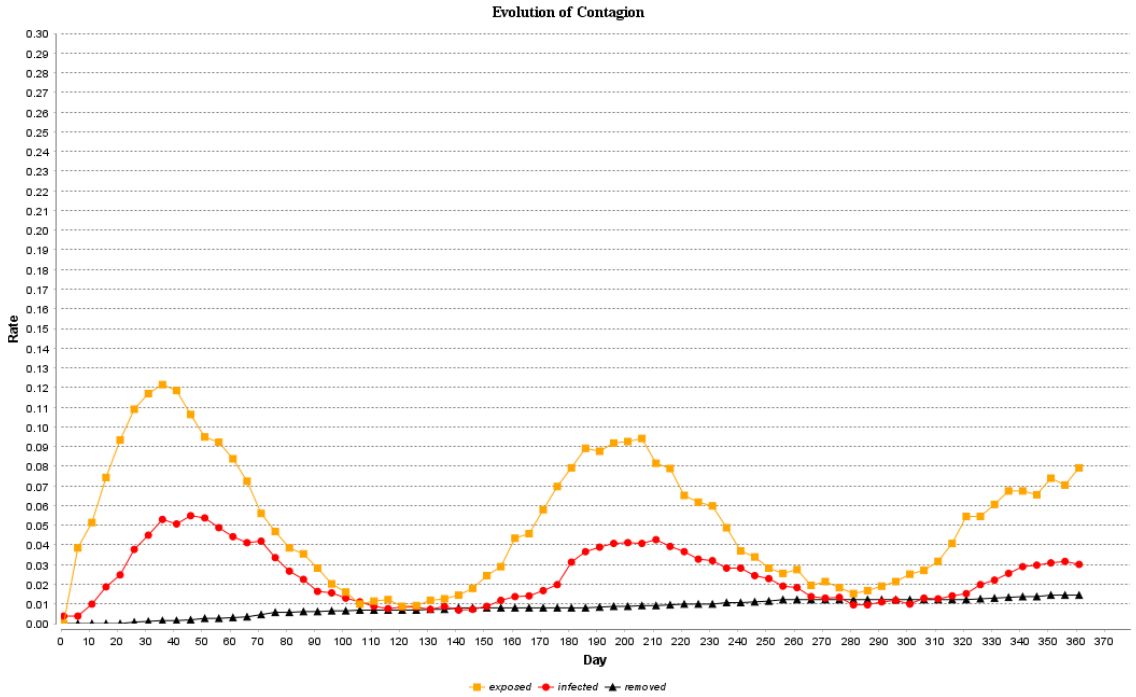

Figure 5.11: Plot showing the exposed, infected and removed curves for the propagation of COVID-19 disease under total lockdown and mandatory use of face masks.

Figure 5.11 presents the epidemic curve when there is an implemented total lockdown and mandatory use of face masks inside prison facilities. The number of cases rapidly rise until it reached its infection rate peak on day 47 at 4.76%. This infection rate is 1.16% lower than only implementing the use of face masks and also indicates a 10.29% decrease from the experiment when no protocols are implemented. It can be seen that the infection rate declined from day 47 until it reached its lowest point and stabilized for 45 days before surging up again. Compared to the plot of the baseline model, the infection curve for this model has lower peaks and has a period for which the infection rate maintains its low values before escalating again into a second wave with a lower peak.

The plot shows a defined bell curve rather than a flattened curve which indicates that the transmission of the virus is still proliferating but only inside the prison cells. Since there are no policies that would restrict the movement of the PDLs inside the prison cells yet, the PDLs are constantly moving and interacting within their cells. Repeated peaks

on the epidemic curve are still expected until another health protocol inside the prison cells is administered.

Limiting PDL Movement Activity

More than the health strategies on mandatory use of face masks and total lockdown, this study considers limiting the movement of PDLs within their prison cells. To magnify the effect of this strategy, there will be no lockdown implemented for this experiment. The model assumes that there is only a 50% chance that an PDL will change its position in the simulation space.

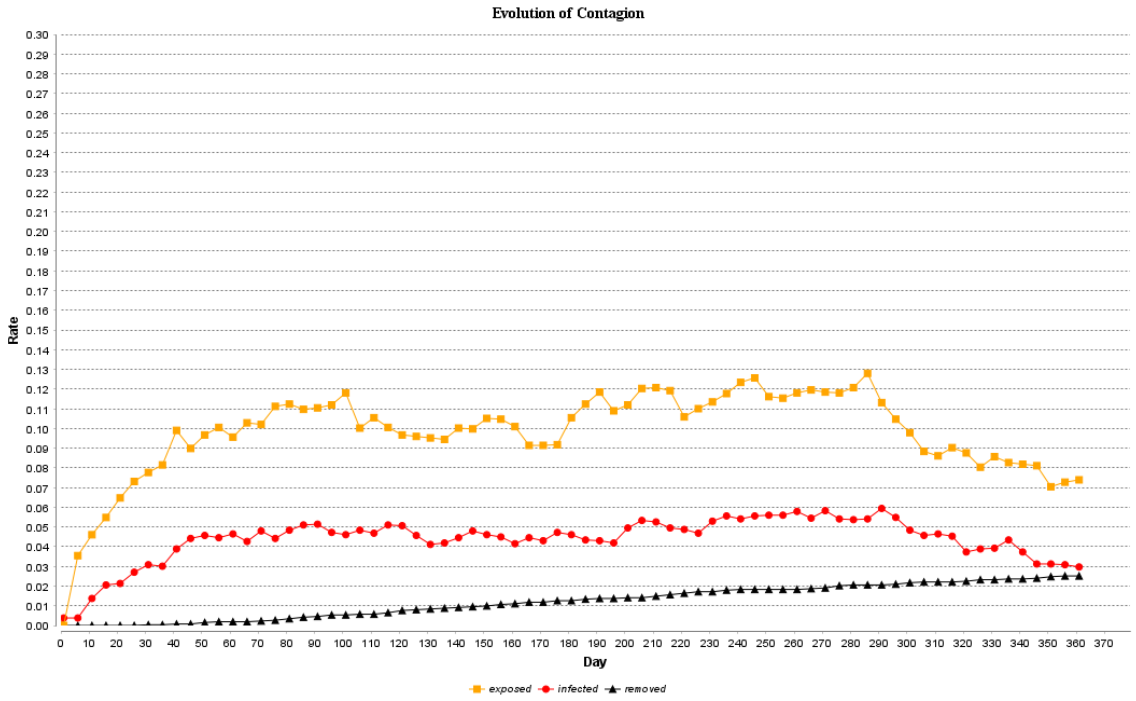

Figure 5.12: Plot exposed, infected and removed curves under mandatory face mask and limited movement protocols.

Figure 5.12 illustrates the epidemic curve when protocols for limiting the movement of the PDLs and the use of face masks are administered in the facility. The plot appears to be a continuous source epidemic curve that rises rapidly from day 1 until it stabilizes throughout the simulation. This plateau curve indicates that exposure to the virus is not confined to one point in time. Since there are still no boundaries for the PDLs to move

at, except possibly the entire correctional facility, the cases are spread over a greater period of time.

The highest infection rate for this simulation is 6.01% which is 9.04% lower than the infection rate in the baseline model. This maximum infection rate value was recorded on day 292. In contrast to previous propagated epidemic curves where there are higher peaks and the graphs can determine the time interval for the peaks and declines of infection rates, the highest infection rate in this simulation is expected in an undetermined interval of time because of its continuity.

5.3 Recommended Protocols to Stabilize the COVID-19 Outbreak

This study aims to generate an appropriate set of strategies for the mitigation of the spread of the COVID-19 virus inside Philippine prisons. Thus, the model combines the recommended strategies from the previous section to generate an environment where the spread of the infection is alleviated. For this experiment, the model assumes that there is a mandatory use of face masks in which all PDLs are properly, a total lockdown is imposed, and the PDLs are limited to move within their prison cells by 50%.

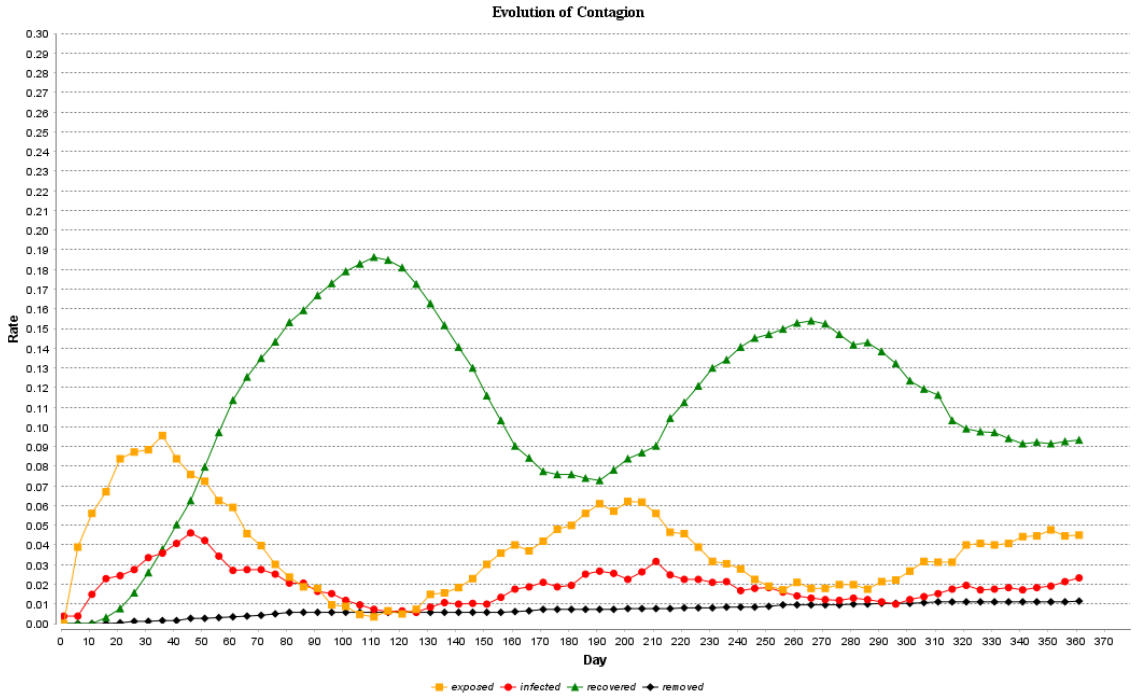

Figure 5.13: Plot showing the exposed, infected, recovered and removed curves under the NPIs including mandatory use of face masks, total lockdown and limited movement of PDLs.

Figure 5.13 presents the epidemic curve when all the discussed nonpharmaceutical interventions are placed. The plot presents three major peaks which are all relatively low. At the start of the simulation, the number of infected cases rises until day 45 at 4.04% which subsequently declines to 0.01% on day 121. Notice that the succeeding waves are lower and stabilized. Though the number of exposed PDLs is relatively higher, the use of face masks helps in lowering the PDLs' risk of contracting the disease. The death rate by the end of the year is listed at 0.01% which is significantly reduced compared to the reported death rate in 2020 by the Bureau of Corrections which is at 2.22%.

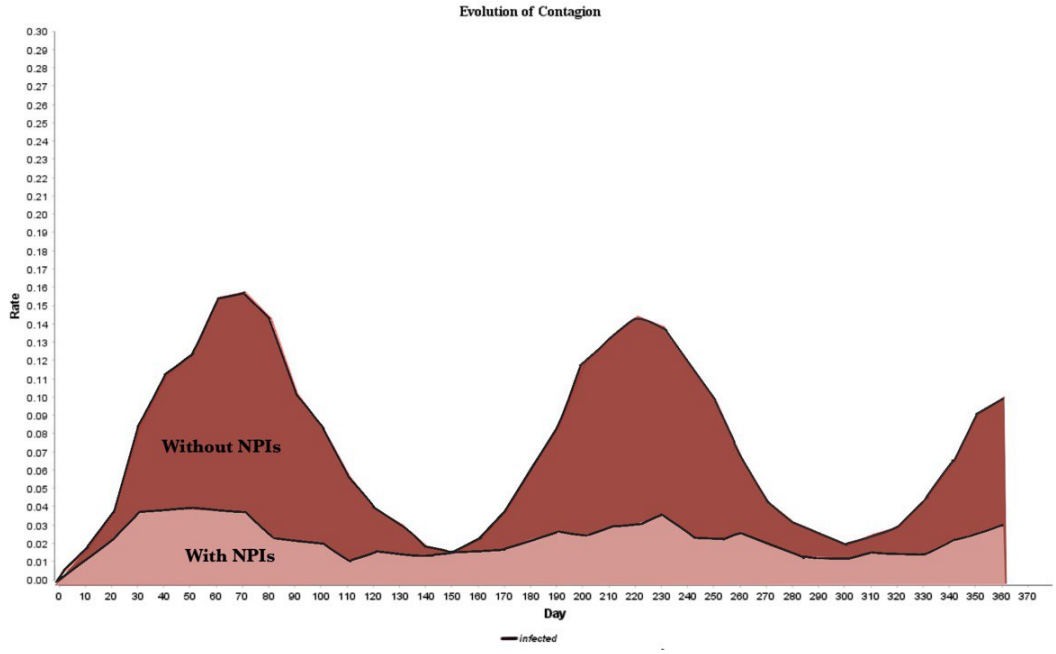

Figure 5.14: Plot showing the difference in the infection curves when there are no NPIs implemented and the following NPIs are administered: mandatory use of face mask, total lockdown, and limited PDL activity.

Figure 5.14 summarizes the impact of the nonpharmaceutical interventions on the propagation of the COVID-19 virus inside the highly congested Philippine prisons. The average maximum infection rate when no public health protocols are implemented is 15.05% which usually peaks in the first quarter of the year. Repeated waves of rapid increase in the rate of infections followed by rapid declines due to immunity from recent infections are anticipated. On the other hand, when there are implemented health protocols inside the facility, the infection rate is at 11.01%, which is 73.15% lower than the infection rate on the baseline model. The number of infected cases rises in the first month of the epidemic but eventually decreases and stabilizes at lower rates in the succeeding months. Additional peaks are expected however not as high and rapid.

Chapter 6

Conclusion and Recommendation

The challenge of high congestion rates in Philippine prisons requires extensive resources to resolve. Thus, in times of an epidemic, an appropriate synthesis of health protocols must be implemented. Using the implemented SEIR model, this study founds that reducing face masks reduces the chances of getting infected by 39.33%. Moreover, a total lockdown must be strictly administered. If this is not possible, the findings of this study suggest that at most 5% of the prison population must be allowed to move along the hallways for a short amount of time which must also be scheduled. These lockdown policies, including the use of face masks, reduce the infection rates by 10.29% to 9.52%. Finally, limiting the activity or movement of the PDLs by 50% can significantly reduce the infection rate by 9.04%. Integrating all of these nonpharmaceutical interventions together results in an 11% decrease in the expected infection rate. These protocols stabilize the infection rates to lower levels until a pharmaceutical solution such as vaccines is accessible.

For the next study, it is recommended to work on other existing communicable diseases that currently plague Philippine prisons such as tuberculosis and viral hepatitis. It is also recommended to add complexities to the model by adding other health interventions or creating a more complex simulation network for more detailed and precise research findings.

List of References

[1] A. * See, *Before covid-19, philippine jails already a death trap*, (2020).

[2] M. Abboah-Offei, Y. Salifu, B. Adewale, J. Bayuo, R. Ofosu-Poku, and E. B. A. Opare-Lokko, *A rapid review of the use of face mask in preventing the spread of covid-19*, International journal of nursing studies advances, 3 (2021), p. 100013.

[3] . B. R. Agrawal, A., *Probability of COVID-19 infection by cough of a normal person and a super-spreader*, Physics of Fluids, (2021).

[4] M. J. Akiyama, A. C. Spaulding, and J. D. Rich, *Flattening the curve for incarcerated populations—covid-19 in jails and prisons*, New England Journal of Medicine, 382 (2020), pp. 2075–2077.

[5] N. Askitas, K. Tatsiramos, and B. Verheyden, *Lockdown strategies, mobility patterns and covid-19*, arXiv preprint arXiv:2006.00531, (2020).

[6] I. Ayouni, J. Maatoug, W. Dhouib, N. Zammit, S. B. Fredj, R. Ghammam, and H. Ghannem, *Effective public health measures to mitigate the spread of covid-19: a systematic review*, BMC public health, 21 (2021), pp. 1–14.

[7] C. E. Baclig, *TIMELINE: One year of COVID-19 in the Philippines*, (2020).

[8] D. Basas and A. Rubin, *Human rights centers management offices*, (2021).

[9] A. W. Byrne, D. McEvoy, A. B. Collins, K. Hunt, M. Casey, A. Barber, F. Butler, J. Griffin, E. A. Lane, C. McAloon, et al., *Inferred duration of infectious period of sars-cov-2: rapid scoping review and analysis of available evidence for asymptomatic and symptomatic covid-19 cases*, BMJ open, 10 (2020), p. e039856.

[10] M. B. Cahapay, *National responses for persons deprived of liberty during the covid-19 pandemic in the philippines*, Victims & Offenders, 15 (2020), pp. 988–995.

[11] N. L. C.-H. H. Y.-J. H. C.-J. C. Y.-J. Chang, H.-J.; Huang, *The impact of the SARS epidemic on the utilization of medical services: SARS and the fear of SARS*, Am. J. Public Health, (2004).

[12] E. Frias-Martinez, G. Williamson, and V. Frias-Martinez, *An agent-based model of epidemic spread using human mobility and social network information*, in 2011 IEEE third international conference on privacy, security, risk and trust and 2011 IEEE third international conference on social computing, IEEE, 2011, pp. 57–64.

[13] N. M. Gharakhanlou and N. Hooshangi, *Spatio-temporal simulation of the novel coronavirus (covid-19) outbreak using the agent-based modeling approach (case study: Urmia, iran)*, Informatics in Medicine Unlocked, 20 (2020), p. 100403.

[14] he Manila Times, *Prisoners need medical intervention, not release*, (2020).

[15] N. Hoertel, M. Blachier, C. Blanco, M. Olfson, M. Massetti, M. S. Rico, F. Limosin, and H. Leleu, *A stochastic agent-based model of the sars-cov-2 epidemic in france*, Nature medicine, 26 (2020), pp. 1417–1421.

[16] E. Hunter and J. D. Kelleher, *A framework for validating and testing agent-based models: a case study from infectious diseases modelling.*, (2020).

[17] E. Hunter, B. Mac Namee, and J. D. Kelleher, *A taxonomy for agent-based models in human infectious disease epidemiology*, Journal of Artificial Societies and Social Simulation, 20 (2017).

[18] ——, *A comparison of agent-based models and equation based models for infectious disease epidemiology.*, in AICS, 2018, pp. 33–44.

[19] N. Imai, K. A. Gaythorpe, S. Abbott, S. Bhatia, S. van Elsland, K. Prem, Y. Liu, and N. M. Ferguson, *Adoption and impact of non-pharmaceutical interventions for covid-19.*, Wellcome Open Res, 5 (2020), p. 59.

[20] J. G. Kahambing, *Philippine prisons and 'extreme vulnerability'during covid-19*, Journal of Public Health, 43 (2021), pp. e285–e286.

[21] K. M. Khalil, M. Abdel-Aziz, T. T. Nazmy, and A.-B. M. Salem, *An agent-based modeling for pandemic influenza in egypt*, Handbook on Decision Making: Vol 2: Risk Management in Decision Making, (2012), pp. 205–218.

[22] M. Khan, S. F. Adil, H. Z. Alkhathlan, M. N. Tahir, S. Saif, M. Khan, and S. T. Khan, *Covid-19: a global challenge with old history, epidemiology and progress so far*, Molecules, 26 (2020), p. 39.

[23] R. O. Macalinao, J. C. Malaguit, and D. S. Lutero, *Agent-based modeling of covid-19 transmission in philippine classrooms*, Frontiers in Applied Mathematics and Statistics, 8 (2022), p. 57.

[24] M. Mahmood, N.-U.-A. Ilyas, M. F. Khan, M. N. Hasrat, and N. Richwagen, *Transmission frequency of covid-19 through pre-symptomatic and asymptomatic patients in ajk: a report of 201 cases*, Virology Journal, 18 (2021), pp. 1–8.

[25] S. Merler, M. Ajelli, L. Fumanelli, M. F. Gomes, A. P. y Piontti, L. Rossi, D. L. Chao, I. M. Longini, M. E. Halloran, and A. Vespignani, *Spatiotemporal spread of the 2014 outbreak of ebola virus disease in liberia and the effectiveness of non-pharmaceutical interventions: a computational modelling analysis*, The Lancet Infectious Diseases, 15 (2015), pp. 204–211.

[26] T. Mitze, R. Kosfeld, J. Rode, and K. Wälde, *Face masks considerably reduce covid-19 cases in germany*, Proceedings of the National Academy of Sciences, 117 (2020), pp. 32293–32301.

[27] B. of Corrections, *Revised IRR of Republic Act No. 10575*.

[28] B. of Jail Management and Penology, *BJMP PROFILE*.

[29] I. C. of the Red Cross, *Covid-19: Lessons from philippines jails show how to fight infectious coronavirus disease*, (2020).

[30] J. Oh, H.-Y. Lee, Q. L. Khuong, J. F. Markuns, C. Bullen, O. E. A. Barrios, S.-s. Hwang, Y. S. Suh, J. McCool, S. P. Kachur, et al., *Mobility restrictions were associated with reductions in covid-19 incidence early in the*

pandemic: evidence from a real-time evaluation in 34 countries, Scientific reports, 11 (2021), pp. 1–17.

[31] U. N. O. on Drugs and Crime, *Position paper: Covid-19 preparedness and responses in prisons*, 2020.

[32] A. Parrocha, *Use of face masks now required in all areas under ECQ*, 2020.

[33] F. Patinio, *CBCP backs release of vulnerable inmates amid health crisis*, (2020).

[34] Z. Y. Peng Y, *Is novel coronavirus disease (COVID-19) transmitted through conjunctiva?*, J Med Virol, pp. 1408–1409.

[35] N. Perra, *Non-pharmaceutical interventions during the covid-19 pandemic: A review*, Physics Reports, 913 (2021), pp. 1–52.

[36] N. Petrosillo, G. Viceconte, O. Ergonul, G. Ippolito, and E. Petersen, *Covid-19, sars and mers: are they closely related?*, Clinical microbiology and infection, 26 (2020), pp. 729–734.

[37] J. Quesada, A. López-Pineda, V. Gil-Guillén, J. Arriero-Marín, F. Gutiérrez, and C. Carratala-Munuera, *Incubation period of covid-19: A systematic review and meta-analysis*, Revista Clínica Española (English Edition), 221 (2021), pp. 109–117.

[38] E. Rafferty, W. McDonald, W. Qian, N. D. Osgood, and A. Doroshenko, *Evaluation of the effect of chickenpox vaccination on shingles epidemiology using agent-based modeling*, PeerJ, 6 (2018), p. e5012.

[39] B. Roche, J. M. Drake, and P. Rohani, *An agent-based model to study the epidemiological and evolutionary dynamics of influenza viruses*, BMC bioinformatics, 12 (2011), pp. 1–10.

[40] L. B. Rodda, J. Netland, L. Shehata, K. B. Pruner, P. A. Morawski, C. D. Thouvenel, K. K. Takehara, J. Eggenberger, E. A. Hemann, H. R. Waterman, et al., *Functional sars-cov-2-specific immune memory persists after mild covid-19*, Cell, 184 (2021), pp. 169–183.

[41] A. Santos, *Waiting to die': Coronavirus enters congested philippine jails*, Al Jazeera News, (2020).

[42] A. B. See, *How covid-19 cases exploded in prisons: A timeline*, (2020).

[43] M. S. Shamil, F. Farheen, N. Ibtehaz, I. M. Khan, and M. S. Rahman, *An agent-based modeling of covid-19: validation, analysis, and recommendations*, Cognitive computation, (2021), pp. 1–12.

[44] J. She, J. Jiang, L. Ye, L. Hu, C. Bai, and Y. Song, *2019 novel coronavirus of pneumonia in wuhan, china: emerging attack and management strategies*, Clinical and translational medicine, 9 (2020), pp. 1–7.

[45] W. G. C. X. e. a. Shi, Y., *A An overview of COVID-19*, 2020.

[46] P. C. Silva, P. V. Batista, H. S. Lima, M. A. Alves, F. G. Guimarães, and R. C. Silva, *Covid-abs: An agent-based model of covid-19 epidemic to simulate health and economic effects of social distancing interventions*, Chaos, Solitons & Fractals, 139 (2020), p. 110088.

[47] A. Staffini, A. K. Svensson, U.-I. Chung, T. Svensson, et al., *An agent-based model of the local spread of sars-cov-2: Modeling study*, JMIR medical informatics, 9 (2021), p. e24192.

[48] C. Sun and Z. Zhai, *The efficacy of social distance and ventilation effectiveness in preventing covid-19 transmission*, Sustainable cities and society, 62 (2020), p. 102390.

[49] G. Suryawanshi, V. Madhavan, A. Mitra, and P. P. Chakrabarti, *City-scale simulation of covid-19 pandemic & intervention policies using agent-based modelling*, in 2021 Winter Simulation Conference (WSC), IEEE, 2021, pp. 1–12.

[50] T. M. D. H. M. G.-A. W. B. T. A. H.-J. T. N. G. S. Van Doremalen, N.; Bushmaker, *Aerosol and surface stability of SARS-CoV-2 as compared with SARS-CoV-1*, N. Engl. J. Med, (2020), p. 1564–1567.

[51] T. P. Velavan, *A mathematical theory of communication*, The COVID-19 epidemic, (2020), pp. 278–280.

[52] Y. Wang, H. Xiong, S. Liu, A. Jung, T. Stone, and L. Chukoskie, *Simulation agent-based model to demonstrate the transmission of covid-19 and effectiveness of different public health strategies*, Frontiers in Computer Science, (2021), p. 82.

[53] H. R. Watch, *Philippines: Reduce Crowded Jails to Stop COVID-19*, (2020).

[54] F. Ying and N. O'Clery, *Modelling covid-19 transmission in supermarkets using an agent-based model*, Plos one, 16 (2021), p. e0249821.

[55] Y. Zhou, L. Li, Y. Ghasemi, R. Kallagudde, K. Goyal, and D. Thakur, *An agent-based model for simulating covid-19 transmissions on university campus and its implications on mitigation interventions: a case study*, Information Discovery and Delivery, 49 (2021), pp. 216–224.

Appendix A

Table for Prison Congestion

PDL PROFILE
STATISTICS 1990-2022

YEAR	POPULATION	% INCREASE	AUTHORIZED CUSTODIAL POSITIONS	RATIO CO: PDL	NO. OF FILLED CUSTODIAL POSITIONS	ACTUAL RATIO CO: PDL	ADMISSION	RELEASES	ESCAPES	RETRIEVAL	DEATHS	APPROPRIATION (P)	PER CAPITA SUBSISTENCE (INMATE/DAY)
1990	13,624	5.04%	1,461	1: 9	1,358	1: 30	4,530	2,969	579	374	138	186,650,000	20.00
1991	14,447	6.04%	1,461	1: 10	1,358	1: 32	4,330	3,225	387	343	132	221,690,000	20.00
1992	15,814	9.46%	1,461	1: 11	1,359	1: 35	4,381	3,215	419	264	122	254,970,000	20.00
1993	16,314	3.16%	1,461	1: 11	1,334	1: 37	4,814	3,129	323	284	139	244,218,000	20.00
1994	17,315	6.14%	1,461	1: 12	1,308	1: 40	4,445	3,448	260	189	131	262,432,000	20.00
1995	17,850	3.09%	1,461	1: 12	1,082	1: 49	4,298	3,574	216	150	163	310,432,000	20.00
1996	18,747	5.03%	1,461	1: 13	1,188	1: 47	4,000	2,776	184	174	174	435,218,000	20.00
1997	20,172	7.60%	1,461	1: 14	1,245	1: 49	4,101	2,526	88	88	128	512,379,000	25.00
1998	20,619	2.22%	1,461	1: 14	1,268	1: 49	4,840	4,270	56	11	156	612,161,000	30.00
1999	21,708	5.28%	1,461	1: 15	1,268	1: 51	5,103	4,147	64	20	141	640,181,000	30.00
2000	23,508	8.29%	1,461	1: 16	1,249	1: 56	4,872	2,798	106	78	144	666,897,000	30.00
2001	23,965	1.94%	1,461	1: 16	1,256	1: 57	4,696	3,992	128	80	210	649,240,000	30.00
2002	25,002	4.33%	1,461	1: 17	1,254	1: 60	4,478	3,325	87	45	223	715,844,000	30.00
2003	26,792	7.16%	1,461	1: 18	1,078	1: 74	4,734	2,907	117	70	278	740,128,000	30.00
2004	28,530	6.49%	1,461	1: 20	1,238	1: 69	4,752	2,867	64	55	261	740,128,000	30.00
2005	29,818	4.51%	1,461	1: 20	1,253	1: 71	5,175	3,831	63	54	268	822,716,000	35.00
2006	30,798	3.29%	1,461	1: 21	1,268	1: 73	5.024	3,683	59	56	291	822,716,000	40.00
2007	32,314	4.92%	1,461	1: 22	1,336	1: 73	5,220	3,391	55	47	354	1,004,152,000	40.00
2008	34,547	6.91%	1,461	1: 24	1,308	1: 79	5,496	3,241	64	37	376	1,030,410,000	50.00
2009	35,934	4.01%	1,461	1: 25	1,385	1: 78	5,461	3,620	67	34	434	1,372,929,000	50.00
2010	35,937	0.01%	1,461	1: 25	1,334	1: 81	5,038	4,342	58	30	440	1,399,853,000	50.00
2011	36,295	1.00%	1,711	1: 64	1,642	1: 66	4,738	4,132	68	43	469	1,510,626,000	50.00
2012	37,251	2.63%	2,211	1: 51	1,550	1: 72	5,506	4,183	81	54	455	1,553,030,000	50.00
2013	38,575	3.55%	2,211	1: 52	1,868	1: 62	5,871	4,147	49	47	510	1,772,015,000	50.00
2014	40,745	5.63%	2,211	1: 55	1,908	1: 64	5,235	2,379	17	22	641	1,885,351,000	50.00
2015	41,432	1.69%	2,211	1: 56	2,037	1: 61	5,096	4,100	18	25	587	1,868,055,000	50.00
2016	41,426	-0.01%	2,211	1: 56	1,976	1: 63	5,955	5,132	17	13	633	1,985,876,000	50.00
2017	42,172	1.80%	2,211	1: 57	1,896	1: 67	5,674	5,418	16	8	655	2,167,600,000	60.00
2018	45,431	7.73%	2,593	1: 53	2,505	1: 54	9,052	5,254	12	10	601	2,664,385,000	60.00
2019	49,420	8.78%	2,593	1: 57	2,484	1: 60	10,049	6,110	16	15	754	4,099,807,000	70.00
2020	48,264	-2.34%	3,593	1: 40	3,177	1: 46	3,528	3,659	2	11	1,082	4,244,182,000	70.00
2021	48,501	0.49%	4,593	1: 32	3,666	1: 40	5,877	4,610	6	10	1,166	3,590,440,000	70.00
December 2022	50,126	3.35%	5,589	1: 27	5,176	1: 29	8,113	6,324	7	17	925	5,264,109,000	70.00

Prepared by:

CSOI Tracy Lyn F. Caabay

Noted:

LORNA D. ALCANTARA
Chief, Planning & Statistics Division

STATISTICS ON PRISON CONGESTION
As of December 2020

PRISON FACILITIES	LAND AREA (Has.)	No. of Buildings	Total Floor Area (Sq.m.)	Actual Floor Area (Sq.m.)	PDL POPULATION	CAPACITY	OCCUPANCY RATE (%)	CONGESTION RATE (%)
New Bilibid Prison					**28,456**			
North					*3,480*			
South					*6,363*			
East	254.73	33	37,807.72	30,246.18	*4,993*	*6,435*	442%	342%
West					*4,235*			
Minimum					*1,486*			
Medium					*7,800*			
Military Camp					*99*			
CIW-Mandaluyong	15.00	7	5,920.00	4,736.00	**3,311**	*1,008*	329%	229%
Iwahig Prison & Penal Farm	26,629.54	15	3,966.00	3,172.80	**2,739**	*675*	406%	306%
Davao Prison & Penal Farm		18	7,954.00	6,363.20	**6,408**	*1,354*	473%	373%
CIW-Mindanao	9,923.64	4	600.00	480.00	**544**	*102*	533%	433%
San Ramon Prison & Penal Farm	664.68	19	4,309.00	3,447.20	**2,208**	*733*	301%	201%
Sablayan Prison & Penal Farm	8,327.40	19	5,841.40	4,673.12	**2,573**	*994*	259%	159%
Leyte Regional Prison	861.60	10	3,991.78	3,193.42	**2,025**	*679*	298%	198%
TOTAL	**46,661.59**	**125**	**70,389.90**	**56,311.92**	**48,264**	**11,981**	**403%**	**303%**

**The land area where CIW is situated belongs to DSWD and was not included in computation of the total land area. (Capacity was adjusted base on the submitted updated TFA of the OPFFs except for NBP)*

**BPM_PSD/ABM_tfc 2019*

AFA = TFA-(TFA*0.2)

Capacity = AFA/4.7

Congestion = [(Population-Capacity)/Capacity]*100

Occupancy rate = (Population/Capacity)*100

Where: **TFA**=Total Floor Area

AFA=Actual Floor Area

Constant **0.2 or 20%** for hallway & comfortrooms

4.7 is the ideal bed capacity

Prepared by:

CSOI Tracy Lou F. Caabay

Noted:

LORNA D. ALCANTARA
Chief, Planning & Statistics Division

Appendix B

Table for Baseline Values

Table B.1: 30 runs with Baseline Values

Highest Infection Rate	Difference between exposure to infection rate	Day
15.15	2.19	68
13.93	3.06	59
19.88	3.86	61
14.66	4.5	60
19.95	0.7	60
12.95	2.8	46
13.3	2.36	47
16.68	4.7	60
12.49	4.07	45
15.55	2.1	51
16.67	0.4	63
15.58	2.32	53
14.01	1.4	76
17.00	3.1	48
12.9	1.04	54
14.42	3.3	69
15.34	1.6	61
17.47	1.1	51
15.15	2.4	64
16.03	3.4	59
14.16	2.8	68
13	4.8	48
17.8	5.2	58

Highest Infection Rate	Difference between exposure to infection rate	Day
14.6	5.08	48
15.36	0.6	44
13.83	0.4	68
12.75	2.4	54
13.13	4	68
16.29	4.6	56
12.33	2	48
14.31	1.68	58

Appendix C

Table for Use of Facemasks

Table C.1: 30 runs with Mandatory Use of Face Masks

Highest Infection Rate	Difference between exposure to infection rate	Day
7.8	8.9	59
8.6	6.1	76
7.5	7.4	87
10.4	6.4	81
8.5		
7.2		63
9.5	8.02	67
10.93	6.5	74
9.5	6.9	79
8.6	7.5	98
8.7	9.4	55
8.7	6	103
8.4	7.7	60
8.7	7.7	93
7.9	6.7	107
10.28	5.3	100
9.1	6.9	76
10.01	7.66	54
8.4	6.1	84
9.3	6.87	66
10.62	8.52	78
9.06	7.5	91
8.83	6.7	69
8.75	6.46	67
7.8	8.3	83

Highest Infection Rate	Difference between exposure to infection rate	Day
10.2	6.9	89
11.38	4.8	68
8.3	6.4	60
10.39	5.9	88
8.49	5.02	88
10.23	7.4	67
8.3	5.7	92

Appendix D

Table for 50% Mutation Rate

Table D.1: 30 runs with Recommended NPIs

Highest Infection Rate	Day
4.04	59
3.6	76
4.5	87
4.4	81
5.5	63
3.5	67
4.93	74
4.5	79
4.6	98
3.7	55
3.7	103
4.4	60
4.7	93
3.9	107
5.28	100
4.1	76
4.01	54
5.4	84
4.3	66
3.62	78
5.06	91
4.83	69
4.75	67
3.8	83

Highest Infection Rate	Day
4.2	89
4.38	68
4.3	60
5.39	88
3.49	88
3.23	67
4.3	92

Appendix E

Source Code

```
/**
* AN ANALYSIS OF THE EFFECT OF HIGH CONGESTION RATES
* IN PHILIPPINE PRISONS ON SARS-CoV-2 PROPAGATION USING
* SEIR AGENT-BASED MODELING APPROACH
* Author: Chien Carisse P. Fernandez
* Tags: SEIRD Model, ABM, COVID-19 Transmission
*/
model Model
global {
    int init_pop <- 679;
    file hallways_shapefile <- file("../includes/Leyte-hallway.shp");
    file cells_shapefile <- file("../includes/Leyte-prison-cells.shp");
    int total_pop <- init_pop update: init_pop - removed;
    float wandering_rate <- 1.0;
    float using_face_mask_rate <- 0.0;
    int using_face_mask_inmate <- round(init_pop * using_face_mask_rate);
    float positivity_rate <- 0.01;
    int init_infected <- round(init_pop * positivity_rate);
    //int init_infected <- 10;
    int wandering_inmate <- round(init_pop * wandering_rate);
    int maxiter <- 365;
    float lambda <- 0.47;
    geometry shape <- envelope(hallways_shapefile);

/************** INITAL STATE OF THE SIMULATION******************/
    int infected <- init_infected update: inmate count (each.is_infected);
    int susceptible <- init_pop - init_infected update: inmate count (each.is_susceptible);
    int exposed <- 0 update: inmate count (each.is_exposed);
    int recovered <- 0 update: inmate count (each.is_recovered);
    int removed <- 0;
    int cycle_number <-0 update: cycle_number + 1;


    init{
        /* Create the simulation space from the shapefiles */
        create hallway from: hallways_shapefile;
        create prison_cell from: cells_shapefile;
```

```
        /* Create agents and assign location of each randomly */
        create inmate number: init_pop{
            assigned_prison_cell <- one_of(prison_cell);
            location <- any_location_in(assigned_prison_cell);
        }


        /* Assign infection state to infected agents */
        ask init_infected among inmate{
            is_infected <- true;
            is_susceptible <- false;
            is_recovered <- false;
            is_exposed <- false;
        }
        /* Assign the movement status of each agent */
        ask wandering_inmate among inmate{
            can_wander_outside <- true;
        }

        ask using_face_mask_inmate among inmate{
            using_face_mask <- true;
        }
    } // end init


    species hallway{
        aspect geom{
            draw shape color:#antiquewhite border: #black;
        }
    } // end hallway

    species prison_cell{
        aspect geom{
            draw shape color:#white border:#black;
        }
    } // end prison_cell

    /* ****************** BEHAVIORAL RULES ****************** */
    species inmate skills:[moving]{
        bool is_exposed <- false;
        bool is_infected <- false;
        bool is_recovered <- false;
        bool is_susceptible <- true;
        bool can_wander_outside <- false;
        bool is_wandering_outside <- false;
        bool using_face_mask <- false;
        int infection_duration <- 0;
```

```
int infection_period;
int recovered_duration <- 0;
int recovered_period;
int incubation_duration <- 0;
int incubation_period;
float speed <- rnd(0.0, 5.0);
prison_cell assigned_prison_cell;
float distance <- 0.0;

reflex wander{
    if flip(1.0){ // can change the value of flip()
        if (can_wander_outside = false){

            speed <- rnd(0.0,1.0);
            do wander bounds:assigned_prison_cell;

    } else {

            speed <- rnd(0.0,1.0);
            do wander;
    }
    }
}


/* Function for probability of infection */
float inf(float n){
    float inf <- (((-18.19 * ln(n)) + 43.276) / 100);
    return inf;

} // end inf

reflex get_infected when:(is_exposed and incubation_duration = incubation_period){
    float r <- rnd(0.000,1.000);
    float fcn_value <- inf(distance);

    if(using_face_mask = true){
        fcn_value <- fcn_value - (fcn_value * lambda);
    }

    if(r < fcn_value){
        is_exposed <- false;
        is_infected <- true;
        infection_period <- rnd(7,18);
    }else{
        is_exposed <- false;
        is_susceptible <- true;
```

```
    }
    distance <- 0.0;
    incubation_duration <- 0;
} // end get_infected

reflex count_incubation_period when: is_exposed{
    incubation_duration <- incubation_duration + 1;
} // end count_incubation_period

reflex get_exposed when: is_infected{
    ask inmate at_distance 1.5 #m{
        if is_susceptible{
            is_exposed <- true;
            is_susceptible <- false;
            incubation_period <- 6;

            // measure the distance of the susceptible
            // agent from the infected one
            distance <- self distance_to myself;
        }
    }
} // end get_exposed


reflex count_infection_duration when: is_infected{
    infection_duration <- infection_duration + 1;
} // end count_infection_duration

reflex remove_or_recover when:is_infected {
    if (infection_duration = infection_period){
        if ( rnd (0.000,1.000) <= 0.0224){
            removed <- removed + 1;
            do die;

        } else {
            is_recovered <- true;
            is_infected <- false;
            recovered_period <- 100; //100 days of immunity
        }
        infection_duration <- 0;
    }

} // end remove_or_recover

reflex count_recovered_days when: is_recovered{
    recovered_duration <- recovered_duration + 1;
} // end count_recovered
```

```
    reflex get_susceptible when: is_recovered{
        if recovered_duration = recovered_period{
            is_recovered <- false;
            is_susceptible <- true;
            recovered_duration <- 0;
        }
    } // end get_susceptible


    aspect appearance{
        if is_susceptible{
            draw circle(0.4) color: #blue;
        }
        if is_exposed{
            draw circle(0.4) color: #orange;
        }
        if is_infected{
            draw circle(0.4) color: #red;
        }
        if is_recovered{
            draw circle(0.4) color: #green;
        }
    }

}//end inmate


float susceptible_rate <- 1.0  update:susceptible/init_pop;
float exposure_rate update:exposed/init_pop;
/* CALCULATE THE HIGHEST RECOVERY RATE */
int highest_recovery_rate_day <- 1;
float recovery_rate update:recovered/init_pop;
float highest_recovery_rate <- 0.0;
reflex recovery_rate when: recovery_rate > highest_recovery_rate{
    highest_recovery_rate <- recovery_rate;
    highest_recovery_rate_day <- cycle_number;
}


/* CALCULATE THE HIGHEST INFECTION RATE */
int highest_infection_rate_day <- 1;
float infection_rate update:infected/init_pop;
float highest_infection_rate <- 0.0;
reflex infection_rate when: infection_rate > highest_infection_rate{
    highest_infection_rate <- infection_rate;
    highest_infection_rate_day <- cycle_number;
```

```
    }

    /* CALCULATE THE HIGHEST DEATH RATE */
    float death_rate update:removed/init_pop;
    float highest_death_rate <- 0.0;
    reflex death_rate when: death_rate > highest_death_rate{
        highest_death_rate <- death_rate;
    }

    /* CALCULATE AVG DIFFERENCE BETWEEN EXPOSURE RATE AND INFECTION RATE */
    float exposure_to_infection <- exposure_rate - infection_rate update: exposure_rate - infection_rate;
    float avg_exposure_to_infection <- 0.0;
    reflex calculate_mean{
        avg_exposure_to_infection <- (avg_exposure_to_infection + exposure_to_infection) / 2;
    }


    /* ENDING CONDITION */
    reflex end_simulation when: cycle_number = maxiter{
        do pause;
    }

}
/************* EXPERIMENTS ************/
experiment map_only type:gui{

    parameter "Wandering rate" var: wandering_rate ;
    output{


        monitor "Initial Population" value: init_pop;
        monitor "Current Population" value: total_pop;
        monitor "Number of infected agents" value:infected;
        monitor "Number of susceptible agents" value:susceptible;
        monitor "Number of recovered agents" value:recovered;
        monitor "Number of removed agents" value:removed;
        monitor "Highest infection rate" value: highest_infection_rate;
        monitor "Highest infection rate day" value: highest_infection_rate_day;
        monitor "Highest recovery rate" value: highest_recovery_rate;
        monitor "Highest recovery rate day" value: highest_recovery_rate_day;
        monitor "Average exposure to infection" value: avg_exposure_to_infection;
        monitor "Exposure to infection" value:exposure_to_infection;



        /* CREATION OF GRAPH */
        display SEIR type: java2D refresh: every(5 #cycles) {
```

```
            chart "Evolution of Contagion" type: series
            x_label: "Day"
            y_label: "Rate"
            x_tick_line_visible: false
            y_range: [0,0.35] // can be modified depending
                              // maximum rate

            {

                // data "susceptible" value: susceptible_rate color: #blue ;
                data "exposed" value: exposure_rate color: #orange;
                data "infected" value: infection_rate color: #red;
                //data "recovered" value: recovery_rate color: #green ;
                data "removed" value: death_rate color: #black ;

            }
        }
    }
}// END OF CODE
```